

Characterisation of a novel bioactive strontium-based endodontic sealant

Dr Sheena Parekh

BDS (QMUL), MFDS (Glasg)

Student number: 120003439

Supervisors:

Professor Robert Hill and Professor Samira Al-Salehi

Submitted in partial fulfilment of the requirements for the Doctorate of Clinical

Dentistry in Endodontics

Queen Mary University, London

Section 1 - Acknowledgements

I would like to express my sincere gratitude to my supervisors Professor Al-Salehi and Professor Hill for their continuous support, supervision, guidance, patience and understanding.

I would also like to thank Dr Benjamin and the team at Coltene Whaledent for their support in the research, providing samples of Guttaflow Bioseal® and incorporating the novel strontium-based bioactive glass within their polydimethylsiloxane matrix.

I would like to thank my colleague and friend Dr Abdullah Alenezi for his continuous support and motivation during the course.

I would like to thank all the staff at the Mile End laboratory, including the manager, Shameem, for her continuous support in managing all the equipment and materials. I would like to show my gratitude to Mr Thomas Kelly for running the ICP-OES data.

I will always praise and forever be grateful to my parents, brother and fiancé for their continuous moral support and well wishes throughout this time, without which I would never have got this far.

Section 2 - Table of contents

2. TABLE OF CONTENTS

1. Acknowledgements	1
2. Contents	2
3. List of figures and tables	6
3.1 List of figures	6
3.2 List of tables	9
4. Abbreviations	10
5. Abstract	12
6. Introduction	14
6.1 Research motive	14
6.2 Pathophysiology of endodontic disease	15
6.3 Aims of root canal therapy	17
6.4 Bioactive materials and its application in Dentistry	17
6.5 Endodontic applications of bioactive materials	19
7. Literature Review	22
7.1 Endodontic sealants – advantages and limitations	22
7.12 Zinc oxide Eugenol based sealants	23
7.13 Calcium hydroxide based sealants	24
7.14 Glass ionomer based sealants	25
7.15 Silicone based sealants	26
7.16 Epoxy resin-based sealants	26
7.17 Tricalcium silicate-based sealants	27
7.18 Methacrylate resin-based sealants	27

7.19 Summary of current endodontic sealants	28
7.2 Development of a bioactive glass	28
7.3 Network connectivity	29
7.4 Mechanism of action of a bioactive glass	30
7.5 Effects of various ions on the bioactivity of a glass	31
7.51 Sodium	31
7.52 Fluoride	32
7.53 Strontium	32
7.54 Phosphate	32
7.6 Methods of preparation for a bioactive glass	33
7.7 Experimental techniques	33
7.71 X-Ray diffraction	34
7.72 Fourier transform infrared spectroscopy	35
7.73 Scanning electron microscopy and energy dispersive X-ray	35
7.74 Inductively coupled plasma optical emission spectrometry	36
7.8 Literature review on Guttaflow Bioseal®	36
7.81 Physical and Chemical properties of Guttaflow Bioseal®	36
7.82 Bioactivity of Guttaflow Bioseal®	37
7.83 Cytotoxicity of Guttaflow Bioseal®	38
8. Aims and Objectives	39
8.1 Aims	39
8.2 Objectives	39

8.3 Null hypotheses	40
9. Materials and Methods	41
9.1 Design of the novel Strontium bioactive glass	41
9.2 Preliminary pilot study	43
9.3 Characterisation of Gutttaflow Bioseal®	45
9.4 Physical properties assessment	50
9.41 Flow value	50
9.42 Radiopacity	51
9.43 Setting time	53
9.44 Solubility	54
9.5 Ion release and characterisation of both sealants after immersion	55
9.51 Preparation of immersion media	55
9.512 Tris buffer solution preparation	55
9.513 Simulated body fluid solution preparation	56
9.52 Immersion media investigations	56
9.521 pH analysis	57
9.522 Inductively coupled plasma optical emission spectroscopy analysis	58
9.523 Fourier transform infrared spectroscopy analysis	59
9.524 X-Ray diffraction analysis	60
9.525 Scanning electron microscopy and energy dispersive X-ray analysis	60
10. Results	62

10.1 Physical properties	62
10.11 Flow value	62
10.12 Solubility	65
10.13 Radiopacity	66
10.14 Setting time	67
10.2 Chemical properties	
10.21 pH changes	70
10.211 pH changes in simulated body fluid	70
10.212 pH changes in tris buffer solution	70
10.22 Ion release	71
10.23 Apatite formation	74
11. Discussion	76
11.1 Discussion of results with comparison to previous studies	76
11.2 Limitations of the study	80
12. Conclusion and recommendations	81
12.1 Conclusion	81
12.2 Recommendations	83
13. References	85
14. Appendices	97

SECTION 3

SECTION 3.1 - LIST OF FIGURES

- **Figure 1** - A) Mixed glass particles placed in a platinum crucible, B) Crucible placed into an electric furnace at 1490°C for 1 hour, C) Resulting melt is rapidly quenched.
- **Figure 2** - A) The glass is milled in the Gyro Mill machine, B) The glass is then sieved, using the Motorised Sieve Shaker, into fine 38 micron particles, C) Fine particles demonstration.
- **Figure 3** - Fourier transform infrared spectroscopy (FTIR) analysis for the novel strontium bioactive glass after 24 hours immersion in artificial saliva
- **Figure 4** - X-Ray Diffraction patterns demonstrating the non-immersed novel bioactive glass (blue line), 7 days immersion in Tris buffer solution (gray line) and 7 days immersion in Simulated body fluid (orange line). The highlighted peaks correspond to apatite formation.
- **Figure 5** - FTIR characterisation comparing GFBS and light bodied silicone material
- **Figure 6** - XRD characterisation of GFBS. The blue reference points superimposed on the x-axis are zirconia values that are taken from the standard file for zirconia from the Joint Committee on Powdered Diffraction Standards. Results show that the high intensity peaks for GFBS match those with the zirconia values.
- **Figure 7** - SEM characterisation of GFBS.

- **Figure 8** - 31 Phosphorus NMR MAS spectrum for GFBS. Graph kindly provided by Dr Harold Toms – NMR facility Manager, QMUL University.
- **Figure 9** - Apparatus required for flow value assessment
- **Figure 10** - Flow value assessment for the endodontic sealant
- **Figure 11** - A) Digital X-Ray machine showing the settings used to expose the radiograph, B) Digital X-Ray machine showing the position of the tube 4.5 cm from the specimen.
- **Figure 12** - A) Apparatus required for setting time assessment. B) The water bath was set for 37 degrees Celsius
- **Figure 13** - Assessment of solubility with the discs immersed in distilled water for 24 hours
- **Figure 14** - Sealant placed in a plastic tube with a conical base. Note, the sealant disc was not placed flat on the tube. This was essential to maximise contact with the immersion solution
- **Figure 15** – A) pH measurement apparatus illustrating the pH calibrating solutions (acid, base and neutral solutions) and the pH measurement device. B) pH measurement of novel sealant after immersion in Tris buffer solution
- **Figure 16** - ICP-OES analysis for the detection of ion release from the endodontic sealants
- **Figure 17** - FTIR analysis using the Spectrum GX (Perkin-Elmer, Waltham, MA, USA)
- **Figure 18** - pH changes in SBF solution for GFBS and the novel sealant
- **Figure 19** – pH changes in Tris buffer solution for GFBS and the novel sealant
- **Figure 20** – A) Ca ion release in SBF, B) P ion release in SBF, C) Si ion release in

- **Figure 21** - A) Ca Ion release in Tris buffer solution, B) P Ion release in Tris buffer solution, C) Si Ion release in Tris buffer solution, D) Na Ion release in Tris buffer solution
- **Figure 22** – Sr ion release in A) SBF and B) Tris buffer solution
- **Figure 23** - Na Ion release analysis against square root time
- **Figure 24** – XRD analysis of GFBS after a 3-month immersion period in SBF. The highlighted areas demonstrate weak intensities for apatite formation.
- **Figure 25** – XRD analysis of the novel sealant after a 3-month immersion period in SBF and TBS

SECTION 3.2 - LIST OF TABLES

- **Table 1** – ideal properties of a root canal sealant
- **Table 2** - Composition (mol%) of the bioactive glass present in the novel strontium sealant and 45S5
- **Table 3** - Flow value assessment samples for GFBS
- **Table 4** - Flow value assessment samples for the novel strontium sealant
- **Table 5** - Solubility testing results for the GFBS and novel sealant.
- **Table 6** - Radiopacity values for GFBS. Three discs for each sealant has been exposed 6 times.
- **Table 7** - Radiopacity values for GFBS. Three discs for each sealant has been exposed 6 times.
- **Table 8** - Guttaflow Bioseal Setting Time Assessment
- **Table 9** - Novel Strontium Sealant Setting Time Assessment

SECTION 4 - LIST OF ABBREVIATIONS

BAG – bioactive glass

Ca – calcium

CaOH – calcium hydroxide

FTIR – Fourier transform infrared spectroscopy

GFBS – Guttaflow Bioseal

HA – hydroxyapatite

ICP-OES – Inductively coupled plasma optical emission spectroscopy

ISO - International Organization for Standardization

MTA – mineral trioxide aggregate

Na – sodium

P – phosphate

PDMS – polydimethyl siloxane

SBF – Simulated body fluid

SEM-EDX - Scanning electron microscopy and energy dispersive X-ray analysis

Si – silicone

Sr – strontium

TBS – Tris buffer solution

XRD – X-ray diffraction

ZOE – zinc-oxide eugenol

SECTION 5 - ABSTRACT

Aims: The aim of this study was to design and synthesise a novel bioactive endodontic sealant that contains a bioactive glass (BAG) with strontium and fluoride embedded in a polydimethylsiloxane (PDMS) matrix. The physical and chemical properties of this sealant were compared with a commercially available, bioactive, endodontic sealant, Guttaflow Bioseal® (GFBS).

Method: Physical properties were tested for both sealants against the International Organisation for Standardisation (ISO) 6876 and included: radiopacity, solubility, setting time and flow value. Chemical properties were also assessed after immersion of both sealants in simulated body fluid (SBF) and tris buffer solution (TBS). The following were analysed: pH rise, ion release (via inductively coupled plasma optical emission spectrometry (ICP-OES)) and apatite formation (via Fourier-transform infrared spectroscopy (FTIR) and X-Ray Diffraction (XRD)).

Results: Both sealants demonstrated physical properties that met ISO 6876. The novel sealant illustrated improved physical properties (higher radio-opacity, lower solubility, and increased setting time). The rate of the Na⁺ ion release from GFBS was greater than 50 times that of the novel sealant. This explains why the solubility was higher from the GFBS® than from the novel sealant. The flow values for both sealants appeared similar. Both sealants showed an increase in pH over a period of three months, after immersion in solution. A higher pH rise was seen in GFBS®. Both sealants showed ion release (Ca, Na, P and Si), with additional Sr release from the novel sealant. Strontium has been associated with upregulation of osteoblast and

downregulation of osteoclast. GFBS had evidence of apatite formation after a 3-month immersion period in SBF, as seen from XRD analysis.

Conclusion: Both the novel sealant and the GFBS[®] demonstrated bioactive properties with ion release from both sealants and the ultimate formation of apatite from GFBS[®]. The novel sealant showed improved physical properties with the addition of strontium increasing radiopacity and the reduction of sodium in the bioactive glass minimising the solubility of the sealant.

SECTION 6 - INTRODUCTION

6.1 RESEARCH MOTIVE

The ideal endodontic sealant does not exist, as of yet. Different factors can contribute to the failure of endodontic treatment; although, persistent intraradicular bacteria or a subsequent secondary infection are the main causes (Tabassum, 2016). Whilst the aim of root canal treatment is to eradicate microorganisms, the literature has shown complete elimination may not be possible and that some microbes can be present in dentinal tubules and cementum post-treatment (Siqueira and Rôças, 2008). A major limitation with current endodontic sealants is a lack of a fluid tight seal; with subsequent microleakage; which contributes to persistent and secondary infection.

With advancements in material research, it can be possible for a sealant to have bioactive properties as well as having the ability to form a bond at the interface of the obturation material and tooth tissue. This can help to improve the seal and prevent bacterial ingress.

Whilst endodontic treatment, for both primary and re-treatment cases have been shown to have good outcomes; with studies quoting a success rate in the range of 68-94% (Sjogren *et al.* 1990, Ng *et al.* 2011), a major prognostic factor that reduces the endodontic outcome is the presence of a periapical lesion. Therefore, if we can target a sealant to regenerate an osseous defect, we may help to improve the overall outcome.

It would be advantageous to develop an endodontic sealant that can also improve upon the physical and chemical properties of currently marketed sealants and thus help improve success rates. The requirement of such specific sealant requires the

ability of the material to be antibacterial, bond with the obturation material and tooth tissue, provide a good seal, whilst promoting apical healing, via regeneration.

Traditional endodontic sealants are composed of the following base materials; calcium hydroxide, zinc oxide eugenol, resin, silicone and glass ionomer. Disadvantages of such materials include little (or no) antibacterial effect, lack of bonding ability to the obturation material and/or tissue and cytotoxic effects on periapical tissues (Jung *et al.*, 2018) (Poggio *et al.*, 2017). Detailed advantages and limitations of such materials are discussed in the literature review section. Modern advancements to sealants involve the use of calcium silicate base materials and/or bioactive glasses which have been shown to have bioactive properties.

When a bioactive glass is incorporated into other dental materials, such as resin composites and glass ionomer cements, it has shown promising results (Han *et al.*, 2021). Thus, it can be hypothesised that its effects can also help to improve the endodontic sealant properties – both physical and chemical.

This theory will be reviewed, tested, and analysed in this research project.

6.2 PATHOPHYSIOLOGY OF ENDODONTIC DISEASE

Dental caries is a prevalent chronic infection arising from cariogenic bacteria (primarily *Streptococcus Mutans*) (Marsh, 2003). These cariogenic bacteria metabolise sugars to produce acids which demineralise the tooth structure. This results in the pH of the tooth surface to drop to below the critical pH of hydroxyapatite demineralisation (pH of 5.5). If left untreated, advancement of the carious front will lead to pulpal inflammation and infection. A classical study which assessed carious teeth demonstrated that when microorganisms are within 1.1mm of the dental pulp, there are insignificant pulpal changes. However, once the microorganisms are within 0.5mm, the degree of pulpal

pathosis increases (Reeves and Stanley, 1966). Once the pulp becomes irreversibly inflamed, its contents will become necrotic. This compromised necrotic pulpal spaces allow for microbes to flourish. Alternative routes of entry for bacteria into the pulpal space include: trauma, cracks, through exposed dentinal tubules at the cervical root surface, through a concurrent periodontal infection with microbes entering via lateral canals, as well as iatrogenic causes (Siqueira, 2016). The aetiology of bacteria in pulpal infections have been proven in numerous studies, which dates back to the 1960's (Kakehashi *et al.*, 1965; Sundqvist, 1976; Moller *et al.*, 1981). The propagation of bacteria will progress from a coronal to apical direction of the root canal and lead to apical periodontitis. Apical periodontitis is a sequel to endodontic pulpal infection and is defined as the inflammation and destruction of peri-radicular tissues caused by etiological agents of pulpal destruction and infection (Gomes & Herrera, 2018). Microbes or their toxins advance in the periapical region from within the root canal. The host, in response to the insult, stimulates an array of defence mechanisms which results in the destruction of periapical tissues to create a barrier from the noxious stimulus (Braz-Silva *et al.*, 2018). Radiographically, this appears as a defect in the bone at the periapex, with a resultant radiolucent lesion. Histopathologically, the lesion comprises of granulomatous tissue, radicular cyst, abscess, scar tissue or less commonly a lesion of non-odontogenic origin, such as a keratocyst (Dunfee *et al.*, 2006).

6.3 AIMS OF ROOT CANAL THERAPY

Root canal treatment is initiated when the dental pulp has been irreversibly damaged, is necrotic or has been electively devitalised for a restoration to be placed. The loss of the pulp tissue creates a dead space inside the root canals which can be colonised by bacteria. Root canal treatment aims to disinfect this space and shape the root canal to facilitate space for an obturation material. The obturation material prevents re-infection of this space; by providing a good coronal and apical seal.

Root canal obturation is done using a combination of a solid cone gutta percha and a sealing cement, with the gutta percha traditionally occupying most of the canal space. With advancements in sealant materials, root canal sealers are playing a larger role in obturation as they incorporate enhanced properties that allow it to be antimicrobial, thus preventing reinfection as well as being bioactive. Such sealers are being recommended for use with a single gutta-percha standardised cone. It has been shown that such sealants demonstrate improved physio-chemical and biological properties (Nouroloyouni, *et al.*, 2023). In these situations, sealant properties are of utmost value since the obturation will be composed of high sealant volumes.

6.4 BIOACTIVE MATERIALS AND ITS APPLICATION IN DENTISTRY

A biocompatible material is one which can interact with living tissues and not cause adverse effects. When a reaction occurs between the material and a tissue (for example tooth or bone), the material is considered to be 'bioactive.' The term bioactive glass has had several definitions. It was initially described as a material that can form a bond between tissue and material (Hench et al., 1971). In 2018, fifty key opinion leaders discussed the definition and concluded that bioactive materials are better

defined as a material that has components that can dissolve and have an antimicrobial activity (Price et al., 2018).

Bioactive glasses are a bioactive, calcium-silicate based material. It is a well-known and researched material that has proven to have excellent properties for apatite formation and bone regeneration (Bagchi *et al.*, 2014) (Cannino *et al.*, 2021).

An ideal bioactive endodontic sealant can form a bond with dentine which improves the seal and minimises leakage, creates an alkaline pH and has a significant antibacterial effect. In addition, it can also upregulate osteoblast and odontoblastic activity that can facilitate regeneration and inhibit osteoclast activity which prevents bone destruction (Ducheyne *et al.*, 1994).

Bioactive materials have been widely used in Dentistry for several years. Materials, such as glass ionomer cements (GIC) have gained popularity and these cements can release fluoride ions that are replaced by the hydroxyl ions from hydroxyapatite present in dental tissues and form fluorohydroxyapatite crystals (Nejeeb *et al.*, 2016). They are also able to form chemical bonds to tooth structure via carboxylic radicals to calcium ions in dentine and enamel.

More recently, bioactive materials are developed with calcium hydroxide and calcium silicate bases (such as mineral trioxide aggregate). These materials can release calcium hydroxide upon hydration, which is able to induce living cells to form mineralised tissue and therefore aid tissue regeneration. The biocompatibility of such materials have been researched over a long period of time with studies showing osteoblast proliferation when in contact with mineral trioxide aggregate, in addition to increased levels of cytokine production (Koh and Torabinejad, 1999).

6.5 ENDODONTIC APPLICATION OF BIOACTIVE MATERIALS

An endodontic sealant is used to fill voids, lateral canals and accessory canals and obturate areas where the core obturation material cannot infiltrate. Failure to use sealants appropriately can lead to microleakage and may result in the failure of root canal treatment by the clinically undetectable passage of bacteria. In addition to this, current sealants can initiate an unfavourable tissue reaction when extruded (Bernath and Szabo, 2003). Thus, the properties of endodontic sealants play a key role. The most popular endodontic sealers (such as calcium hydroxide, zinc oxide or resin based) can fill voids in canals and exert modest (or no) antibacterial effects. However, they are unable to bond effectively with dentine and promote bone regeneration. The limitation of these sealants necessitates the development of a bioactive sealant. A recent study has shown that whilst periapical lesions show significant healing following non-surgical endodontic treatment (regardless of the type of sealant used), bioceramic and bioactive sealants have demonstrated better results (Khandelwal *et al.*, 2022) (Bardini *et al.*, 2021).

There is a current trend in modern endodontics that is leading towards the regular use of biocompatible, (although more specifically, bioactive) endodontic sealants with an increase in demand for tricalcium silicate-based cements. It is considered that these interact with water (either added to the material) or from fluids within the canal space to form calcium hydroxide (Camilleri, 2011). The ionic dissociation of calcium hydroxide results in the release of calcium and hydroxyl ions. The hydroxyl ions promote an increase in pH (gives rise to antibacterial properties; likely due to protein denaturation and damage to the DNA and cytoplasmic membrane) (Mohammadi & Dummer, 2011). Additionally, the reaction between the released calcium ions and phosphorus (from body fluid) allows for apatite formation (Okiji & Yoshida, 2009).

These sealants are either presented as a powder and liquid formula that is premixed and introduced into the canal via a syringe or they are delivered into the canal using a file/gutta percha point after mixing. Such sealants are water-based and therefore usually cannot be used in warm vertical compaction methods as they can dry out, may not set and reduce the bond strength (DeLong *et al.*, 2015).

As mentioned earlier, bioactive glasses are considered to dissolve and release ions which have proven to be beneficial for healing and repair of endodontic lesions. An example of a recently developed bioactive commercial endodontic sealant is GuttaFlow Bioseal® (GFBS), manufactured by Coltene Whaledent. It is claimed to be a bioactive material that can bond to tooth and gutta percha, expand on curing, and is easy to manipulate. It consists of a bioactive glass and gutta-percha particles embedded within a polydimethylsiloxane (PDMS) matrix. The total volume of the bioactive glass fillers in the product is declared by the manufacturer to range between 5-30% in weight (Hoikkala *et al.*, 2021). GFBS has been shown in the literature to have physical properties in line with the International Organisation for Standardisation Dentistry - Root canal sealing materials 6876 (ISO 6876). However, in comparison to other endodontic sealants, it has a lower radiopacity (Tanomaru-Filho *et al.*, 2017), lacks a fluid tight seal (Lee *et al.*, 2020) and has a short setting time (Gandolfi *et al.* 2016). When assessing GFBS's characteristics, a study showed that GFBS can release ions and form apatite-like morphological structures (Hoikkala *et al.*, 2018). It is also considered to be a bioactive material with one study claiming it promoted wound closure in a concentration dependent manner and that it did not induce apoptosis, thus preserving cell viability (Rodríguez-Lozano *et al.*, 2019). Whilst the composition of the bioactive glass in GFBS is not clearly stated, a study has inferred it to be that of 45S5

(Hoikkala *et al.*, 2018). This implies that the composition of the glass would be 46.1SiO₂, 26.9Na₂O, 24.4CaO, 2.5P₂O₅ in mol %.

The addition of strontium and fluoride in a bioactive glass is thought to have multiple additional benefits. Strontium has been shown to upregulate osteoblast and odontoblastic activity (Gentleman *et al.*, 2010), has the potential to differentiate dental pulp stem cells to induce dentine-like matrix formation (Huang *et al.*, 2016), demonstrate antimicrobial activity against several gram-negative bacteria in a dose dependant manner (Liu *et al.*, 2016), and its high atomic number can help confer radiopacity in the sealant. Having a high strontium content in a fluoride free phosphate glass can reduce or inhibit apatite formation. In the presence of fluoride, strontium does not suppress apatite formation and the formation of an apatite can occur directly without the need for a precursor - octacalcium phosphate (Liu *et al.*, 2016).

An ideal endodontic sealant would therefore contain both strontium and fluoride. It would also have a low sodium content, which will minimise solubility (Wallace *et al.*, 1999) and a high phosphate content which increases apatite formation, supports osteoblast differentiation and osteogenesis (Li *et al.*, 2021).

SECTION 7 - LITERATURE REVIEW

7.1 ENDODONTIC SEALANTS – ADVANTAGES AND LIMITATIONS

Current obturation methods use endodontic sealants to augment the seal between the gutta-percha and dentinal wall. The sealant helps to achieve a three dimensional hermetic seal by filling voids between the main obturation material and dentine as well as accessory canals. Additionally, root canal sealants can serve further functions such as providing antimicrobial properties, act as a lubricant for a core material, increase the radiopacity for a core material and aid in regeneration (Rathi *et al.*, 2020).

In 1982, Grossman published an eleven criteria requirement that an ideal endodontic sealant would need. These are summarised in Table 1.

Table 1 – Ideal properties of a root canal sealant

Grossman (1982) - Ideal properties of a root canal sealant	
1.	The sealant should be tacky when mixed to provide a good adhesion between it and the canal wall when set
2.	The sealant should allow for a hermetic seal
3.	The sealant should be radiopaque to allow for visualisation on a radiograph
4.	The particles of the sealant powder should be very fine so that it can mix easily with the liquid
5.	The sealant should not shrink upon setting
6.	The sealant should not discolour the tooth structure
7.	The sealant should be bacteriostatic or at least not encourage bacterial growth
8.	The sealant should set slowly

9.	The sealant should be insoluble in tissue fluids
10.	The sealant should be well tolerated by the periapical tissues
11.	The sealant should be soluble in common solvents if it is necessary to remove the root canal filling material

Endodontic sealants are most commonly categorised based upon their composition. The following are the categories of current root canals sealants based upon their composition; zinc-oxide eugenol, salicylate, glass ionomer, silicone, resin, tricalcium silicate, dicalcium silicate, methacrylate resin and calcium hydroxide.

A detailed analysis of each sealant type is described below, along with its advantages and limitations.

7.12 Zinc oxide eugenol based sealants

Zinc oxide eugenol (ZOE) based sealants were initially introduced in 1931 (Rickert and Dixon, 1931). They are still very popular and currently in use based on their long-term success. They consist of a zinc oxide powder and eugenol liquid, which, when mixed and placed in the canal forms an amorphous gel, into which residual zinc oxide powder gets embedded. Currently marketed zinc oxide eugenol based sealants include: Pulp Canal Sealer® (Kerr) and Tubli-Seal sealer® (Dentsply Petrópolis Ind, Rio de Janeiro, Brazil). Newer adaptations for endodontic sealants are being manufactured such as Bioseal® (OGNA Pharmaceuticals, Muggio Italy). Bioseal® is a ZOE based sealant with hydroxyapatite added. However, no special therapeutic effects are seen from this, with studies showing no statistically significant difference in the sealing ability of Bioseal® and that of Pulp Canal Sealer® (Gambarini & Tagger, 1996). Advantages of ZOE based sealants include: its antimicrobial properties and

slow setting reaction which allows clinicians with more working time. Disadvantages of ZOE based sealants include its known cytotoxic effect on cell membrane and respiratory functions. Such cytotoxic effects generally last longer than most sealants (Huang *et al.*, 2002). In addition, they have shown to shrink on set, demonstrate solubility and can stain the tooth structure.

7.13 Calcium hydroxide sealants

These sealants were first used for obturation in the 1940s. Advantages of calcium hydroxide based sealants include its ability to stimulate periapical tissues and promote healing along with its antimicrobial properties. The following mechanisms of action has been proposed for the mode of action of calcium hydroxide (Desai and Chandler 2009):

1. Antimicrobial due to the release of hydroxyl ions which raises the pH
2. The raise in pH also allows the material to neutralise the lactic acid from the osteoclast and prevents the dissolution of the mineralised components of teeth.
3. The pH increase also activates alkaline phosphatase which stimulates hard tissue formation.
4. Calcium hydroxide can denature proteins found in the root canal and reduces toxicity.
5. Calcium hydroxide can activate calcium-dependent adenosine triphosphatase reaction associated with hard tissue formation.
6. Calcium hydroxide diffuses through dentinal tubules and can communicate with the periodontal ligament space to arrest external root resorption and accelerate healing.

Examples of calcium hydroxide-based sealants include Sealapex® (Kerr Dental) and Apexit® (Ivoclar Vivadent).

The limitations of calcium hydroxide-based sealants, include eliciting an inflammatory reaction due to its poor seal. The poor seal is attributed to the solubility of the sealant, with a study reporting the presence of the disintegrated sealant particles in macrophage cytoplasm away from the root filling material found in the periapical regions of dogs teeth (Soares *et al.* 1990). The degradation of the sealant and incomplete fill is likely to be the reason for the added inflammatory response seen when using calcium hydroxide-based sealants clinically. Advantages of the sealant, include, the release of free calcium ions which allow for cell migration, differentiation and mineralisation. However, the literature demonstrates that this release is insufficient and that the calcium hydroxide-based sealants had a statistically insignificant effect on healing of apical periodontitis (Waltimo *et al.*, 2001).

7.14 Glass ionomer-based sealants

These sealants are made by mixing fine silicate glass powder with polyacrylic acid. An example of a glass ionomer based endodontic sealant is Ketac-Endo® (3M ESPE, St. Paul, MN, USA). This sealant is only available in some parts of the world, and is less commonly used in comparison with other sealants. Advantages of glass ionomer-based sealants include its ability for molecular adhesion. However, several studies demonstrate that this type of sealant shows significantly more leakage (Ozata *et al.*, 1999), with the leakage pathway most likely being at the dentine-sealer interface (Gee *et al.*, 1994).

7.15 Silicone based sealants

These materials are based on a polymethylvinylsiloxane matrix and sets by an addition reaction between the vinyl groups attached to the polydimethylsiloxane and the hydrosilyl groups to form a polymer. GuttaFlow®, GuttaFlow2® and GuttaFlow Bioseal® (Coltene/Whaledent) are examples of a silicone-based sealant. The literature shows that silicone based sealants do not flow as easily into lateral canals when compared with traditional sealants such as zinc oxide eugenol and resin based sealants (Barbizam *et al.*, 2007). However, the silicone-based sealants demonstrate low solubility, especially when compared with zinc oxide eugenol (Keleş & Köseoğlu 2009) (Yigit & Gencoglu, 2012).

7.16 Epoxy resin-based sealants

These sealants were introduced by Schroeder in 1957 (Schroeder, 1981). They are composed of low molecular weight epoxy resins and amines and set by an addition reaction between epoxide groups and amines to form a polymer. AH 26® and AH Plus® (Dentsply Sirona Konstanz, Germany) are examples of epoxy-based sealants. Advantages of these sealants include its reduced solubility, good apical seal and its micro-retention to the root canal dentine. Whilst the material's low solubility is a big advantage, clinicians need to exercise care when handling the material as extruded sealant generally does not get resorbed. Extrusion into the inferior alveolar canal can result in paraesthesia and pain (Geethapriya *et al.*, 2019). Other disadvantages of the sealant include an acute inflammatory reaction of the mucosa which occurs when in contact with unset paste with resin-based sealants. There have also been reports with local and systemic allergies (Ali *et al.*, 2022).

7.17 Tricalcium silicate-based sealants

These materials have been introduced in the 1990s by Torabinejad. Mineral trioxide aggregate (MTA) is a tricalcium silicate-based material. They are considered to be bioactive due to its ability to release calcium and hydroxyl ions which induces the formation of apatite upon contact with body fluids. Advantages of tricalcium silicate-based materials include an improved seal due to the formation of apatite, antibacterial properties due to a rise in pH values and increase in osmotic pressure (from the ion release) along with its' bioactive and biocompatible properties. Examples of such sealants include: ProRoot MTA Gray® (Dentsply Sirona, Johnson City, TN, USA) and BioRoot RCS® (Septodont). Disadvantages include: slow setting reaction and therefore not a good choice of sealant should a post/core/build-up be required at the same visit.

7.18 Methacrylate resin-based sealants

The latest generation of methacrylate resin-based sealants use a combination of self-activating etchant, primer and sealant. The technique of usage for this sealant includes a 'single cone technique' where the master cone gutta-percha point is embedded within the sealant in the root canal. This allows for an adhesion between the dentine and sealant to allow for a hermetic seal. An example is Metaseal® which is available in a powder-liquid form and can be used either with Resilon® (a dimethacrylate-containing polycaprolactone-based thermoplastic root filling material) or gutta-percha. The advantages of this sealant include the formation of a hybrid dentine which is a good mechanism for bonding. The adhesive mechanism of the methacrylate resin based sealant to radicular dentine is via micromechanical retention of resins that can infiltrate the demineralised collagen matrix. A limitation of this is that effective bonding

in the root canal system can be difficult due to the limited vision and access. Other factors that can limit bonding include the presence of sclerotic dentine in the canals, debris in the canal wall and the high cavity configuration factor (C-factor) inside the long and thin canal wall. These factors can severely reduce the sealing ability (Kim *et al.*, 2010).

7.19 Summary of current endodontic sealants

After conducting a review on the literature, the sealing ability proves to be one of the most important property a sealant can possess. The lowest microleakage is shown amongst the tricalcium silicate sealants (Komabayashi *et al.*, 2020). These sealants also have the most favourable antimicrobial and biocompatibility properties (Komabayashi *et al.*, 2020). Thus, based on these findings, if we can develop a novel bioactive sealant with minimal solubility and possess additional antimicrobial properties, we can try and improve upon the currently available sealants on the market and aim to meet Grossman's ideal sealant property requirement.

7.2 DEVELOPMENT OF THE BIOACTIVE GLASS

As mentioned previously, bioactive has been described as a material that can form a bond between tissue and material (Hench *et al.*, 1971). These materials can release ions and induce the formation of hydroxyapatite when in contact with physiological solutions. The bioactive glass was first introduced by Larry L Hench who intended to develop a graft material compatible for the human body. He realised that hosts rejected implants made of inert metal and plastic materials. Such materials were used mainly for amputation cases from wounded soldiers during the war in Vietnam (Greenspan, 2016). After a discussion with a colonel in the medical command, Professor Hench began researching for materials with a better compatibility. He found

that the host tends to reject materials made of metals and polymers and reasoned that making a calcium phosphate-based material would help in reducing the risk of rejection. This material turned out to be a glass composition that would not be rejected by the body and can also form a bond with living tissue. The material was also able to precipitate hydroxyapatite in aqueous solutions, with the ability of bonding to hard and soft tissues without rejection.

In 2018, 50 key opinion leaders discussed the definition of bioactivity and stated that bioactive materials can be better defined as a material that has components that can dissolve and have antimicrobial activity (Roulet J-F, 2018).

Today, a bioactive glass (BAG) is a well-known and researched material. Bioactive materials may be osteoconductive or osteoinductive. In contrast, bioinert materials do not elicit any specific responses or interact with the biological environment. However, they can result in a foreign-body reaction and the formation of a fibrous capsule. These fibrous capsules can result in micromovements and eventual failure of treatment (Holland *et al.*, 2017).

The first bioactive glass is commercially trademarked as Bioglass[®]45S5. It is composed of 45% SiO₂, 24.5% Na₂O, 24.5% CaO, and 6% P₂O₅ in mol%.

7.3 NETWORK CONNECTIVITY

The network connectivity is essential for designing a bioactive glass as it will determine the overall dissolution and bioactive properties of the final material. Network connectivity is defined as the number of bridging oxygens per silicone.

It is possible to predict the structure of a glass based upon the molar composition (Hill & Brauer, 2011). The structure of a silicate glass is a silica tetrahedron. This is joined to adjacent units by Si-O-Si bonds. These bonds are referred to as bridging oxygen

bonds. In vitreous silica, the tetrahedron is linked by four bridging oxygens. This results in an insoluble glass structure. An example of this is window glass. Addition of non-bridging oxygens will disrupt this insoluble glass structure by replacing the bridging atoms. For a glass to become bioactive, the network connectivity is required to be close to 2, although bioactivity can be present up to a network connectivity of 2.6 (Eden, 2011). Glasses of a low network connectivity have a lower glass transition temperature in addition to being highly reactive, and hence bioactive.

A bioactive glass consists of three components: network formers, network modifiers and intermediate oxides. Network formers can form glasses without the need for additional elements. Silica is an example of a network former. Network modifiers disrupt the glass network structure by breaking the Si-O-Si bond and give rise to non-bridging oxygens. They make a glass more reactive by reducing its stability and allowing it to dissolve faster. Examples of glass modifiers include calcium oxide (CaO) and sodium oxide (Na₂O). Intermediate oxides, such as zinc oxide (ZnO) can act as a network modifier and form a glass structure, only when mixed with glass formers.

The network connectivity of a glass is important to consider when designing new glasses with different compositions for endodontic sealants. Ideally, we would want the network connectivity of the glass to be as close to 2 as possible (and below 2.6).

7.4 MECHANISM OF ACTION OF A BIOACTIVE GLASS

A bioactive glass can form a layer of apatite, allowing the material to bond with bone/tooth structure upon immersion in physiological fluids. Studies have also demonstrated a bioactive glass to form a hydroxyapatite layer after immersion in Tris buffer solution (TBS) and simulated body fluid (SBF). Upon immersion of the bioactive glass in body fluids, exchange of network-modifier ions from the glass (such as

sodium, potassium and calcium) with hydrogen (H^+) or hydronium (H_3O^+) ions, from the body fluid occurs. This results in a breakdown of SiO_2 bonds within the glass structure. This reaction results in a raise in the pH. As the hydroxyl (OH^-) concentration increases, there is a continuation of breakdown between the silicone and oxygen bonds, forming orthosilicic acid, or $Si(OH)_4$ and silanols on the surface of the material. The silanol groups re-polymerise to form a silica rich layer on the surface of the bioglass. This attracts calcium and phosphate ions which crystallise with the surrounding body fluids to create a carbonated hydroxyapatite layer (Takadama *et al.*, 2001).

7.5 EFFECTS OF VARIOUS IONS ON BIOACTIVITY OF A GLASS

The composition and concentration of various ions within a bioactive glass can influence the properties, dissolution and bioactivity of a glass.

7.51 Sodium

Wallace *et al.*, demonstrated that different concentrations of sodium content in a bioactive glass resulted in different properties being present such as the hardness and bioactivity of a glass (Wallace *et al.*, 1999). The study showed that increasing the sodium content, decreased the glass transition temperature and peak crystallisation temperature in a linear manner. The network connectivity of a glass is not affected when the sodium ions are replaced with calcium ions in a glass. However, when the sodium ions are incorporated in a glass, the glass network expands which results in a reduced density of the glass. The study also demonstrated that an increase in the sodium content resulted in an increase in the solubility and subsequent ion release of a glass (Wallace *et al.*, 1999).

7.52 Fluoride

Brauer et al., showed that the addition of fluoride ions in a bioactive glass reduced its glass transition temperature. This meant that the glass showed reduced hardness and was more bioactive (Brauer *et al.*, 2009). In addition to this, the onset of crystallisation and peak temperatures were also reduced when the fluoride content was raised.

7.53 Strontium

Strontium addition has been proven to have several benefits. Firstly, its high atomic number (atomic number of 38, in comparison with calcium, which is 20) allows the material to have an increased radiopacity when exposing dental radiographs (O'Donnell *et al.*, 2010).

Strontium has also shown to have positive effects on bone turnover. It has been introduced by Gentleman et al., in 2010 as a bone regeneration material by substituting strontium for calcium ions on a mol% basis (Gentleman *et al.*, 2010). Another study showed that the substitution of strontium with calcium resulted in an increase in the unit cell volume and density of apatite (O'Donnell *et al.*, 2008). Additionally, the strontium substitution in a bioactive glass can increase the glass density and molar volume without affecting the network structure (Xiang & Du, 2011).

7.54 Phosphate

Varying the phosphate content of a bioactive glass can influence the rate of osteogenesis. A study by Li et al., 2020, showed that a high phosphate content led to increased apatite formation. The likely mechanism for this is due to the physical, chemical and biological functions of phosphorus which include: reducing the pH rise associated with ion exchange during glass degradation, allowing for faster release of

ions, increasing cell viability and alkaline phosphatase activity (ALP activity), promotion of osteogenic and angiogenic gene and protein expression (Li *et al.*, 2020).

7.6 METHODS OF PREPARATION FOR A BIOACTIVE GLASS

Bioactive glasses can be prepared using two methods: melt quench method and sol-gel technique (Kaur *et al.*, 2015). The melt quench method involves mixing the glass powder precursors and melting them at high temperatures. This is followed by rapid cooling and grinding of the obtained glass. The sol-gel method involves the transformation of the precursors into a colloidal gel, followed by solvent removal by heat, then crushing the obtained glass (Deshmukh *et al.*, 2020). Advantages of the sol-gel method include the ability to fabricate a bioactive glass with different porosities. A disadvantage of this preparation method is that it takes longer to process and make the glass (around 2 weeks), and you can get residual hydroxyl (OH⁻) in the glass composition, which prevents one from adding fluorine to the glass as the hydroxyl and fluoride will not react. The melt quench method allows for a better control of glass composition, and is a quicker method used to obtain the glass (Kaur *et al.*, 2015).

7.7 EXPERIMENTAL TECHNIQUES

To assess the composition of the sealant, multiple methods can be used. These include Fourier Transform Infrared Spectroscopy (FTIR), which measures the molecular absorbance of infrared radiation that allows you to calculate the frequency of oscillation for 2 atomic masses bonded in a molecule. This provides a surface analysis of the composition of a material. X-Ray diffraction (XRD) is another method that is based upon the interaction between X-rays and a material, which causes the X-ray to diffract at a particular angle. This allows for a deeper analysis of a material composition and identify its phase. Scanning electron microscopy (SEM) analysis

provides high resolution images of a sample, whilst Energy Dispersive X-Ray Analysis (EDX) can provide elemental identification and quantitative compositional information. Finally, Inductively coupled plasma optical emission spectrometry (ICP-OES) can be used to determine the elemental composition present in a solution.

7.71 X-Ray Diffraction technique

X-ray diffraction technique is based upon the interaction of X-rays with the material. It is used in experimental methods to identify the different phases of a material; it can be used to determine if the bioactive glass is amorphous or crystalline.

X-rays have a short wavelength and are a form of very high energy electromagnetic radiation. The interaction between the X-ray radiation and the crystal lattice structure in atoms causes the X-rays to diffract off at a certain angle. The diffraction angle is described by Bragg's Law of diffraction (Le Pevelen, 2017).

Powdered X-Ray diffraction can be used to identify different phases in a material that has a distinctive peak at a particular 2θ angle. It can also give us a rough estimate of the crystal sizes. Thus the X-Ray diffraction can help to distinguish between amorphous phase where the atoms are disordered in the lattice and the crystal phase where the atoms are arranged in a regular array within the crystal lattice.

For this research project, the X-Ray diffraction can be used to investigate the structure of the original endodontic sealant as well as the apatite formed from the bioactive glasses after immersion in SBF and TBS. It can also identify the crystallographic changes tracked as a function of time, after set immersion intervals.

7.72 Fourier Transform Infrared Spectroscopy (FTIR)

Fourier transform infrared spectroscopy (FTIR) analysis is used to gain an infrared spectrum of absorbance or emission of a material. The technique aims to measure the amount of absorbance by the sample of infrared radiation. The wavelength of the light absorbed by the sample is related to the energy of the light beam which in turn is related to its frequency. The covalent bonds in a molecule will selectively absorb radiation at specific wavelengths. This changes the vibrational energy in the bond. The type of vibration (stretching or bending) induced by the infrared radiation will depend on the atoms that are present in the bond. Since different bonds and functional groups absorb different frequencies, the transmittance pattern is different for different molecules. This technique will help us to identify the type of bonds present within a material and hence the structural phase.

7.73 Scanning electron microscopy (SEM) and Energy Dispersive X-Ray analysis (EDX)

Scanning electron microscopy (SEM) is used to gain a magnified image of the surface of a material using electrons instead of light to form an image. The SEM instrument produces a beam of electrons which follows a vertical path through the microscope and hits the samples. When the electrons hit the sample, the electrons and X-Rays are ejected from the sample. Detectors are used to collect these X-Rays, backscattered electrons and secondary electrons and it converts them into a signal that is sent to a screen to produce the final magnified image. This allows us to assess the composition of the sample.

7.74 Inductively Coupled Plasma Optical Emission Spectrometry (ICP-OES)

Inductively coupled plasma optical emission spectrometry (ICP-OES) is an experimental method used to determine the quantity of elements that are present within a sample. In this method, a source of energy, from heat arising from an argon plasma (operating at 10,000 kelvin) is absorbed by atoms and ions. This causes electrons to move from their original ground state to an excited state. As an electron then returns from its higher energy level to a lower energy level, it emits a particular wavelength of light. The ICP-OES can measure the amount of light being emitted at each wavelength and uses this information to calculate the concentration of an ion in the sample.

7.8 LITERATURE REVIEW ON GUTTAFLOW BIOSEAL®

Guttaflow Bioseal® (GFBS) (Coltene/Whaledent AG, Altstätten, Switzerland), is a polydimethyl siloxane based material which contains gutta-percha powder, bioactive glass ceramic, zirconium dioxide (added for radiopacity), silver (as a preservative), and colouring. It was launched towards the end of 2015 for commercial use worldwide. Studies have shown promising biological, physical and chemical properties of this endodontic sealant.

7.81 Physical and chemical properties of Guttaflow Bioseal®

A study conducted by Lyu *et al.*, in 2022 assessed the physiochemical properties of GFBS® and compared the results with other sealants (IRoot SP®, AH Plus®, RoekoSeal® and GuttaFlow2®). The film thickness, flow, working time and setting time were investigated (Lyu *et al.*, 2022).

The film thickness and flow value for an endodontic sealant are important to assess, as it will determine the ability for a sealant to penetrate the intricate anatomy of root canals. An ideal endodontic sealant would have a low film thickness and high flow value, which can help to obturate anatomical irregularities found within canals. Lyu *et al.*, found that of the 5 tested sealants, GFBS had the highest film thickness (44 μm) and the lowest flow value (21.43 mm). Whilst this is in line with the ISO standards, a sealant would benefit with a higher flow value. This can be done by reducing the ingredient components of the sealant or reducing the particle size of the components.

The working time for GFBS was 4.5 minutes and the setting time was 16.3 minutes. This was the shortest setting time in comparison with the other 5 sealants (Lyu *et al.*, 2022). This short working/setting time will mean that clinicians will have less time to obturate and may increase the pressure during the obturation period. This short working period for GFBS may be explained by its setting reaction, which appears to be a combination of a hydration reaction and a polymerisation reaction. These two reaction mechanisms result in an increase in temperature which in turn will increase the setting reaction speed.

The findings from this recent publication are in keeping with previous in-vitro experimental studies performed by Tanomaru-Filho *et al.*, in 2017 and Camargo *et al.*, in 2017 (Tanomaru-Filho *et al.*, in 2017 and Camargo *et al.*, in 2017).

7.82 Bioactivity of Guttaflow Bioseal®

Hoikkala *et al.*, assessed the dissolution and mineralisation characterisation of GFBS (Hoikkala *et al.*, 2014). Specifically, they looked at mineralisation, pH changes, dissolution and ion release. They found that the GFBS released Ca and Si ions into the surrounding aqueous solution and formed hydroxyapatite like morphological

structures; which had a Ca/P ratio similar to that of crystallised hydroxyapatite. In addition to this, the study demonstrated that the sealant resulted in a pH rise to pH 7.9, which has been known to have feasible antimicrobial levels *in vivo*. Thus, findings from this study demonstrate that GFBS as a sealant has been shown to be bioactive and the promising *in vitro* results can imply a more favourable outcome can be expected *in vivo* for endodontic treatment.

7.83 Cytotoxicity

A study performed by Rodriguez-Lozano *et al.*, in 2019 assessed cell viability (Rodriguez-Lozano *et al.*, 2019). They evaluated cell attachment by placing human periodontal ligament cells onto the material surface and assessed the effects of the GFBS on cementum protein 1 (CEMP1), cementum-derived attachment protein (CAP), bone sialoprotein (BSP), ameloblastin (AMBN), amelogenin (AMELX) and alkaline phosphatase (ALP) gene expression on the periodontal cells. The results found from this experimentation were promising, with more than 90% of viable cells being present from the culture with GFBS[®]. By comparison, AH Plus[®] and MTA Fillapex[®] had a significantly lower level of cell viability and caused membrane permeability-related apoptosis and necrosis. The study also showed that the concentration of the GFBS was important, as the sealer promoted wound closure in a concentration-dependent manner. The findings from this study are consistent with other studies (Saygili *et al.*, 2017, Mar Collado-Gonzalez *et al.*, 2017).

Whilst the results from the literature appear to be promising, further investigation is needed to confirm whether the *in vitro* cementogenic potential can lead to regeneration *in vivo* of the periapical region.

SECTION 8 - AIMS AND OBJECTIVES

8.1 – AIMS:

- To design and synthesise a novel bioactive endodontic sealant that contains a bioactive glass (BAG) with Strontium and Fluoride and high levels of Phosphate
- To investigate and compare the physio-chemical properties of the novel strontium sealant compared to that of a commercial bioactive sealant (Guttaflow Bioseal® (GFBS))
- To explore and investigate the effect of Strontium and Fluoride incorporated in the novel strontium sealant

8.2 – OBJECTIVES:

- To design an experimental bioactive glass, which contains an optimum concentration of different ions (Fluoride, Calcium, Strontium and Phosphate) for incorporation into a polydimethyl siloxane (PDMS) matrix.
- To investigate the bioactivity of the novel strontium sealant and commercial sealant in terms of ability to release Fluoride, Calcium and Phosphate ions and to form apatite after immersion in simulated body fluid (SBF) and Tris buffer solution (TBS).
- To compare the physical properties of the novel strontium sealant and commercial sealant
- To investigate the effect of the addition of Strontium and Fluoride in the composition of the novel strontium sealant.

8.3 – NULL HYPOTHESIS:

There is no difference in the physio-chemical properties between the novel strontium based endodontic sealant and commercially available GFBS.

SECTION 9 - MATERIALS AND METHODS

Two sealants were investigated; an experimental, novel strontium bioactive endodontic sealant and a commercially available bioactive endodontic sealant (Guttaflow bioseal® (GFBS), Coltene Whaledent Ltd (Kendal House, The President Suite - A, Victoria Way, Burgess Hill RH15 9NF). The physical, chemical and biomineralisation properties were assessed and compared.

9.1 DESIGN OF THE EXPERIMENTAL BIOACTIVE GLASS

Based on an ideal criterion for designing bioactive glasses, the following bioactive glass was designed (Table 2) and compared with the 45S5. The novel glass has a network connectivity of 2.28. By comparison, the 45S5 has a network connectivity of 2.11. The network connectivity largely determines the rate of dissolution for a bioactive glass.

Table 2 - Composition (mol %) of the bioactive glass present in the novel strontium sealant and 45S5

	Composition (mol %)					
Glass	SiO ₂	CaO	Na ₂ O	P ₂ O ₅	CaF ₂	SrO
Novel strontium glass	36.0	22.5	7.0	7.0	5.0	22.5
45S5	46.1	26.9	24.4	2.6	0	0

The bioactive glass was prepared via the melt quench technique. In this method, raw powders were weighed and equated to consist of 200 g batches consisting of analytical grade SiO_2 (Prince Minerals Ltd., Stoke-on-Trent, UK), Na_2CO_3 , CaCO_3 , SrCO_3 (on melting, the carbonates of calcium and sodium will evolve carbon dioxide resulting in calcium oxide and sodium oxide), P_2O_5 and CaF_2 (all Sigma-Aldrich, Gillingham, UK) were weighed on a scale with an accuracy of ± 0.01 g. Owing to the hygroscopic nature of P_2O_5 , this powder was added last to the batch. The powders were then mixed vigorously in a sealed container.

The mixed powders were then placed onto a platinum crucible and melted in an electric furnace (EHF 17/3, Lenton, Hope Valley, UK) at 1490°C for 1 hour. The resulting melt was rapidly quenched and the frit was collected and transferred to an oven at 37°C and dried overnight (Figure 1).

After complete drying, the glass frit was placed in a Gyro-mill machine (Gyro mill, Glen Creston, London, UK) for 14 minutes. The milled powder was then sieved using a 38 micron sieve (Endecotts Ltd., London, UK) to obtain a fine particle size, (Figure 2).



Figure 1 – A) Mixed glass particles placed in a platinum crucible, B) Crucible placed into an electric furnace at 1490°C for 1 hour, C) Resulting melt is rapidly quenched.



Figure 2 – A) The glass is milled in the Gyro Mill machine, B) The glass is then sieved, using the Motorised Sieve Shaker, into fine 38 micron particles, C) Fine particles demonstration.

9.2 PRELIMINARY INVESTIGATION AND PILOT STUDY

A preliminary investigation was carried out to ensure that the novel strontium glass was bioactive. 75 mg of the glass was immersed in 50 ml of artificial saliva (AS7) and stored in an incubator (KS 4000i control, IKA) at 37 °C with a 60 rpm agitation. After 24 hours, the BAG powder was collected by passing the solution through a filter paper (qualitative filter paper, VWR, 5-8 micron particle size retention), and dried overnight at 37 °C. The resulting powder was analysed for apatite formation by Fourier transform infrared spectroscopy (FTIR) analysis. The experimental glass demonstrated apatite formation and further analysis was carried out. Figure 3, demonstrates evidence of apatite formation using FTIR analysis. The peak at approximately 1025 cm^{-1} is characteristic of the P-O vibration in apatite, whilst the split peaks at 568 cm^{-1} (illustrating PO_4^{3-} bond) and 601 cm^{-1} (HPO_4^{2-} bond) are also characteristic of apatite.

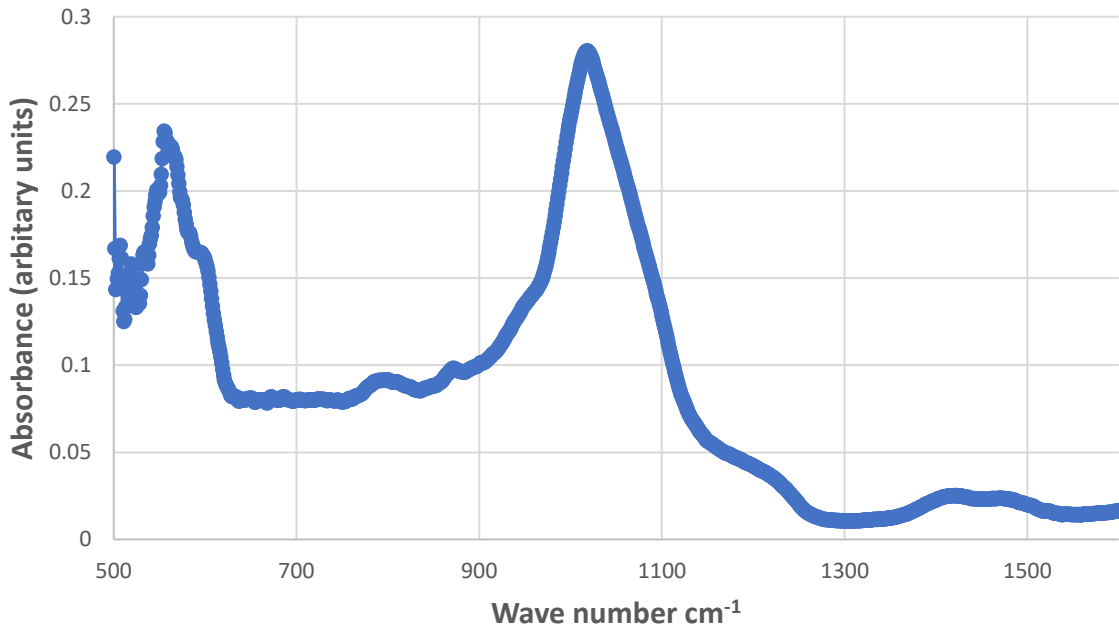


Figure 3 – Fourier transform infrared spectroscopy (FTIR) analysis for the novel strontium bioactive glass after 24 hours immersion in artificial saliva

After conducting this preliminary study, a further pilot experiment was performed to assess for evidence of apatite formation after immersion of the novel strontium bioactive glass in SBF and TBS for 1 week. X-ray diffraction patterns were then assessed to identify apatite formation.

Figure 4, demonstrates the X-ray diffraction pattern obtained. Evidence of apatite was clearly demonstrated after the 7 days immersion from both SBF and TBS. The highlighted peaks correspond to apatite diffraction patterns.

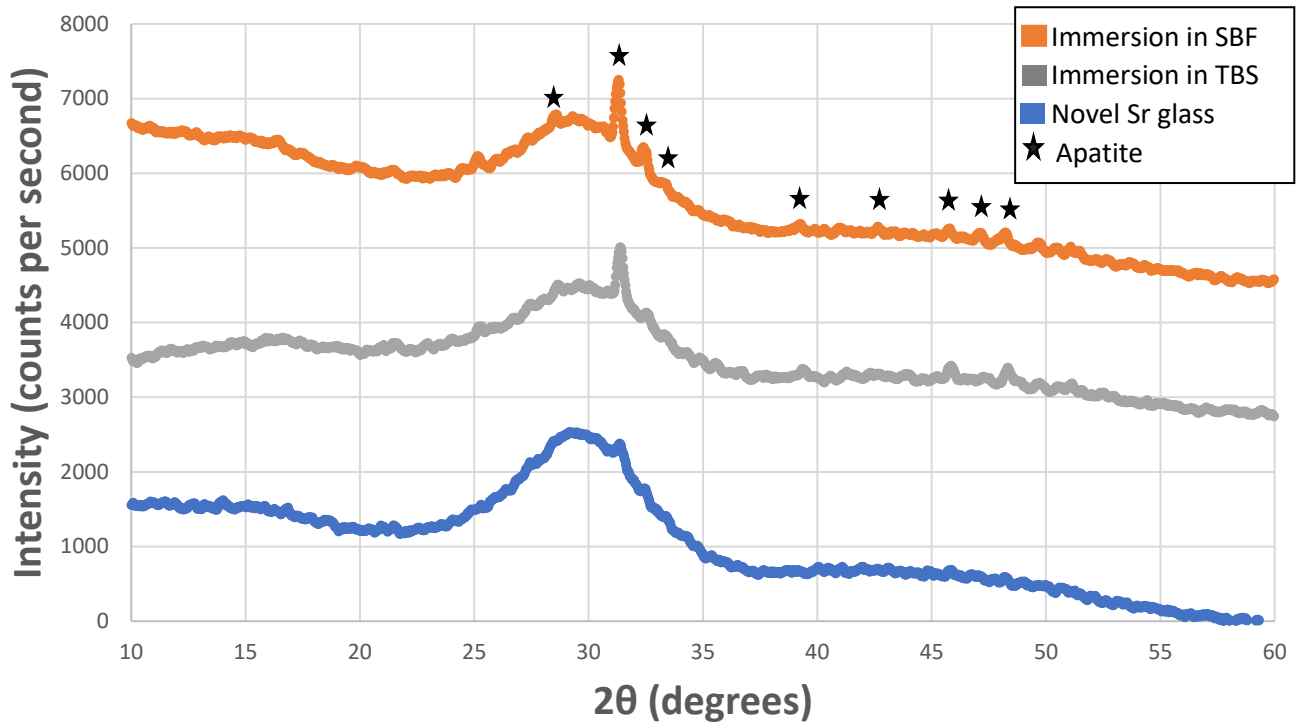


Figure 4 – X-Ray Diffraction patterns demonstrating the non-immersed novel strontium bioactive glass, 7 days immersion in TBS and 7 days immersion in SBF. The highlighted peaks correspond to apatite formation.

9.3 CHARACTERISATION OF THE GUTTAFLOW BIOSEAL®

An initial characterisation test was performed for the GFBS® to identify the composition and structure of the material, as well as the type of bioactive glass.

The FTIR spectra of the GFBS lacked the non-bridging oxygen Si-O-Si stretch (that is typically present in a bioactive glass) at $1039-854\text{ cm}^{-1}$. Instead, the results are in keeping of that of light bodied silicone material, (Figure 5). This can indicate that the silicone material is either masking the bioactive glass particles or that there is very little bioactive glass present in the sealant.

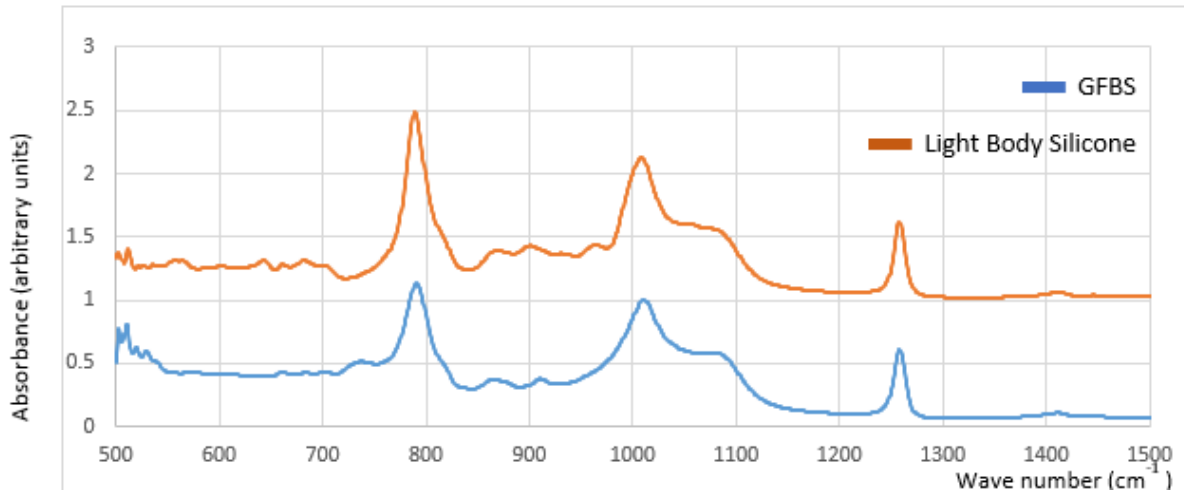


Figure 5 – FTIR characterisation comparing GFBS and light bodied silicone material

XRD results showed sharp crystalline peaks, rather than the expected broad peaks associated with the amorphous glass phase. An explanation for this may be attributed to the zirconia present, which due to its high atomic number, can overshadow the glass particles (Figure 6).

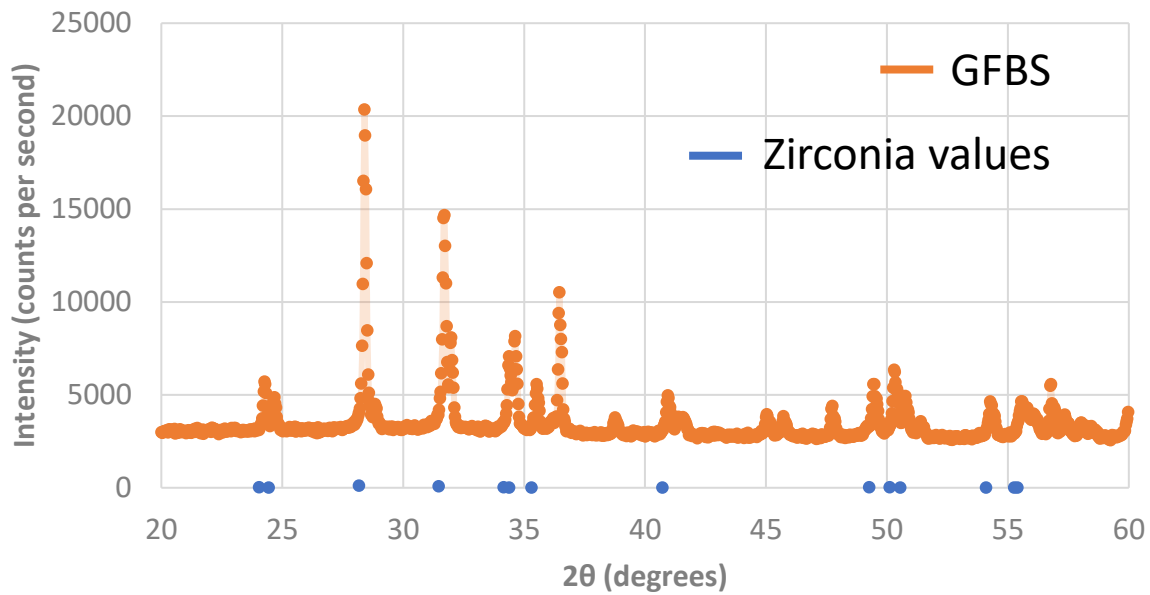


Figure 6 - XRD characterisation of GFBS. The blue reference points superimposed on the x-axis are zirconia values that are taken from the standard file for zirconia from the Joint Committee on Powdered Diffraction Standards. Results show that the high intensity peaks for GFBS match those with the zirconia values

SEM analysis was also conducted to try and identify the bioactive glass in GFBS. The results showed the presence of calcium, sodium, silicone, zinc, zirconia and trace amounts of phosphorus, aluminium and magnesium in the material, (Figure 7).

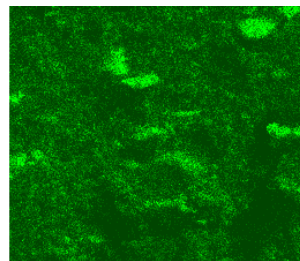
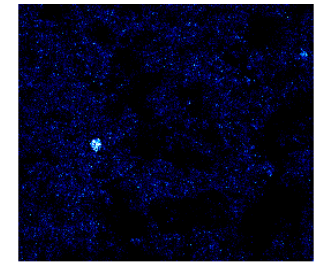
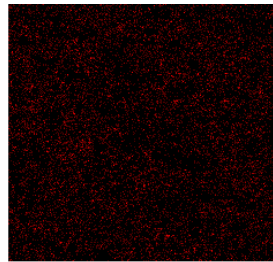
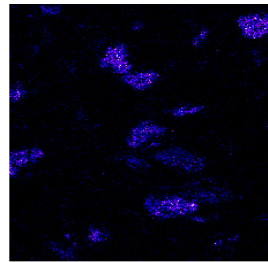
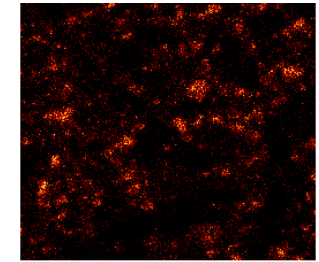
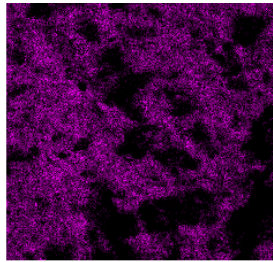
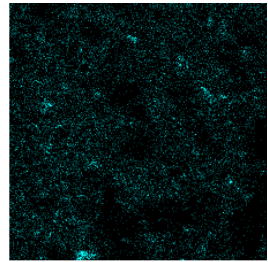
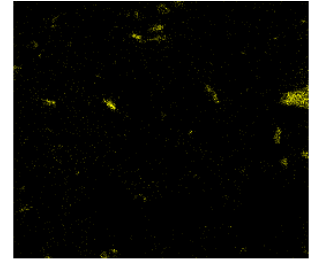
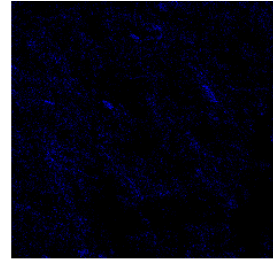
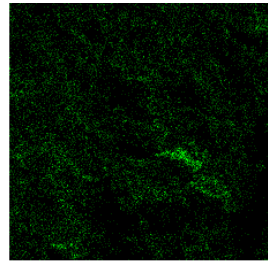
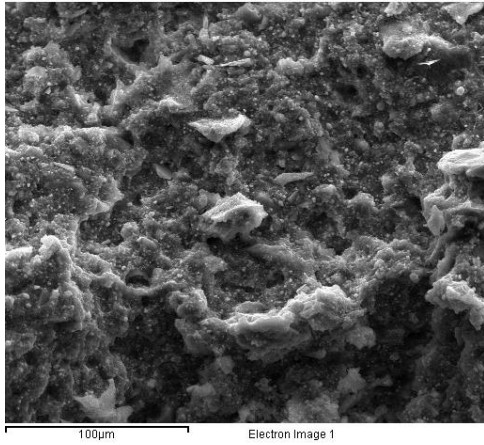


Figure 7: SEM analysis of GFBS.

Finally, a ³¹P magic angle spinning (MAS) nuclear magnetic resonance (NMR) spectra (³¹P MAS NMR) was conducted which demonstrated a peak at -1.99 ppm (Figure 8). This is not in keeping with the expected results as if the glass was 45S5, as previously mentioned in the literature, there would be a peak maximum at 9.0 ppm which would match the coordinate modifier cations (Na²⁺ and Ca²⁺) in 45S5 (Souza *et al.*, 2018).

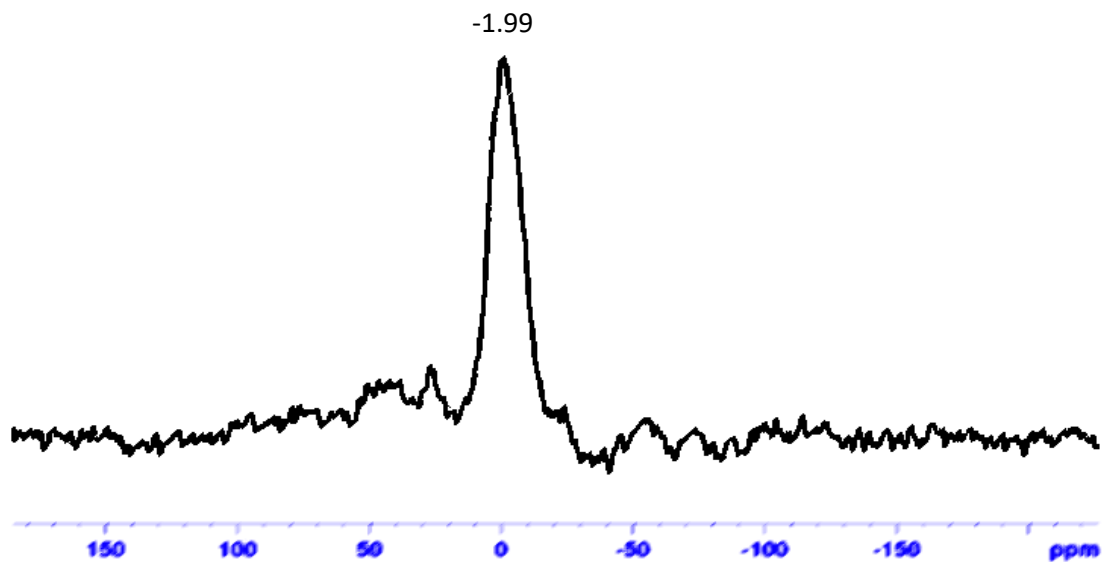


Figure 8: ³¹P NMR MAS spectrum for GFBS. Graph kindly provided by Dr Harold Toms – NMR facility Manager, QMUL University.

None of the above tests for the characterisation of GFBS provided conclusive evidence of the presence of a bioactive glass - assumed to be 45S5 (Hoikkala, 2018).

9.4 PHYSICAL PROPERTIES TESTING

All physical tests were assessed according to and compared with the International Organisation for Standardisation (ISO 6876) to ensure both the novel strontium and GFBS sealant met regulatory requirements for clinical use.

9.41 Flow value assessment

The equipment used to measure flow value, as outlined in the ISO standards, is illustrated in Figure 9.

1. 2 glass plates, measuring 100 mm by 100 mm and 5 mm thick with a mass of 20 g
2. 100 g weight
3. 1 ml graduated syringe
4. Sealant
5. Ruler

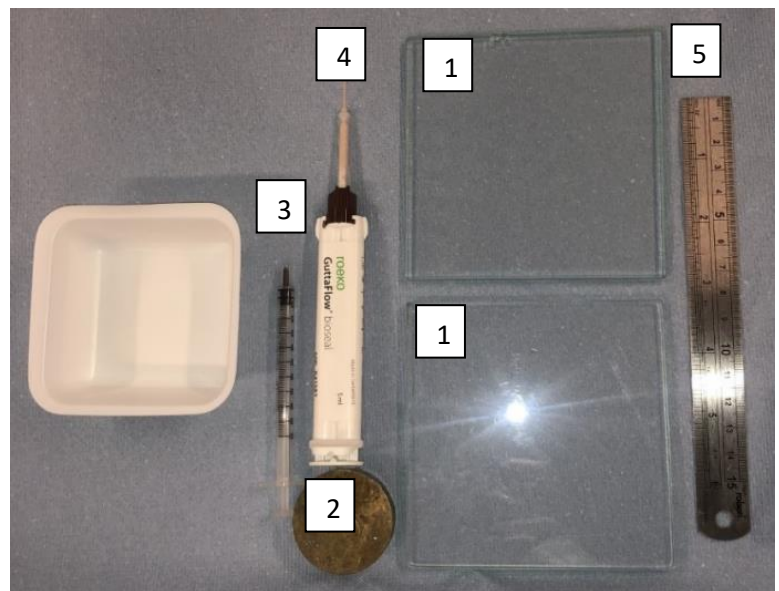


Figure 9 – Apparatus required for flow value assessment

To measure the flow value, 0.05 ml (+/- 0.0005 ml) of mixed sealer was placed on the centre of a glass slab with a graduated syringe, Figure 10a.

After 180 seconds (+/- 5 seconds) from the start of mixing the sealant, the second glass slab was placed on top of the sealant (Figure 10b) and the 100 g weight was added on top of the second glass slab (Figure 10c).

10 minutes (600 seconds) from the start of mixing the sealant, the weight was removed from the top of the second glass slab and the maximum and minimum diameter of the sealant measured (Figure 10d, 10e).

The results were accepted where the diameter was deemed within 1 mm of each other.

The procedure was repeated three times.

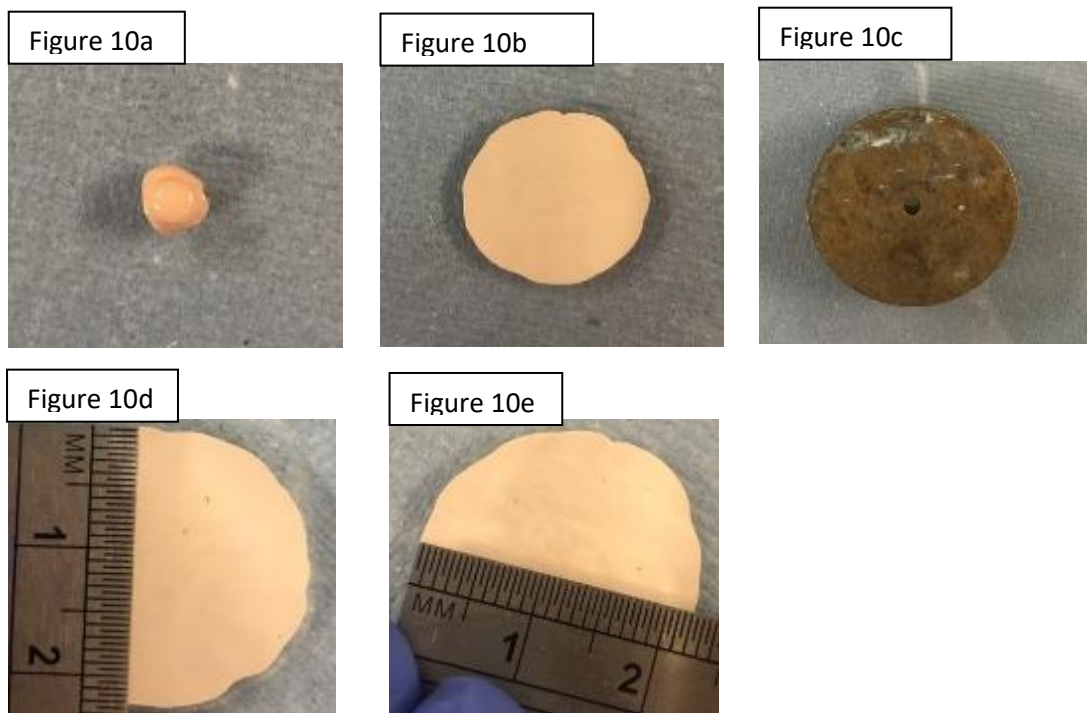


Figure 10 – Flow value assessment for the endodontic sealant

9.42 Radiopacity testing

Specimens ($n=3$) were prepared using circular plastic moulds (10 ± 0.1 mm diameter and 1.0 ± 0.1 mm thickness) for both sealants. The prepared disc samples were placed along with an Aluminium step wedge on a digital radiographic sensor. The Aluminium step wedge was used as a standard for measuring the equivalent radiopacity based on the thickness of the aluminium step wedge. This provides an internal standard for

each digital radiographic image and allowed calculation of the radiopacity of the sample in terms of aluminium thickness.

A digital X-ray machine (Vatech EXdI) with an exposure for 0.10 seconds at 60 kV and 7 mA was used to take the radiograph, (Figure 11a). The distance between the surface of the film and the tube was 45 cm, (Figure 11b).

Analysis of images:

Software Image J was used for image analysis.

Using the software, a rectangular area was drawn on each of the Aluminium wedge, and the relevant grey value was measured. A calibration curve was then plotted for each image showing the Aluminium wedge thickness versus the relevant grey value and a linear regression equation was calculated.

A circular area was drawn on the radiographic image of the disc followed by the relevant grey value measurement.

The equivalent Aluminium thickness (mm) for each sample was calculated using a linear regression equation. This was repeated 6 times for each disc.

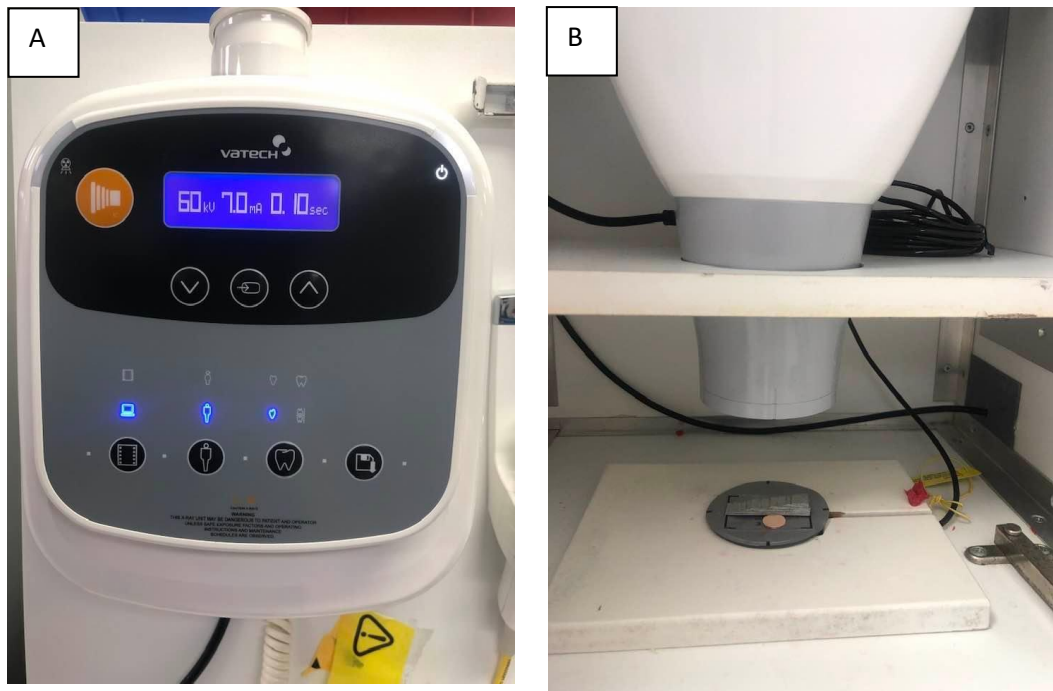


Figure 11 – A) Digital X-Ray machine showing the settings used to expose the radiograph, B) Digital X-Ray machine showing the position of the tube 4.5 cm from the specimen.

9.43 Setting time

Discs were prepared for this purpose (n=3). A Gilmore needle, metal moulds, sealant, glass plate and water bath (Figure 12a) were used for the experimentation. A water bath at 37 °C was prepared and moulds (10 ± 0.1 mm diameter and 1.0 ± 0.1 mm thickness) were placed on top (Figure 12b). Samples were placed on the mould on the glass plate and filled to a level surface with sealer. After 120 ± 10 seconds from the end of mixing, the samples were placed on top of a metal block in a water bath set at 37 °C. When the working time (15 minutes), stated by the manufacturer approached, the Gilmore needle was carefully loaded vertically on to the horizontal surface of the sealant. If an indentation was visible, the needle was raised, the needle tip was wiped

clean and after a minute the needle was lowered to a new position on the surface of the sealer. This was repeated until indentations were no longer visible. The final setting time was recorded as the time from the end of mixing to when no indentations were seen on the surface of the specimen. The experiment was repeated three times and an average setting time was determined for both sealants.

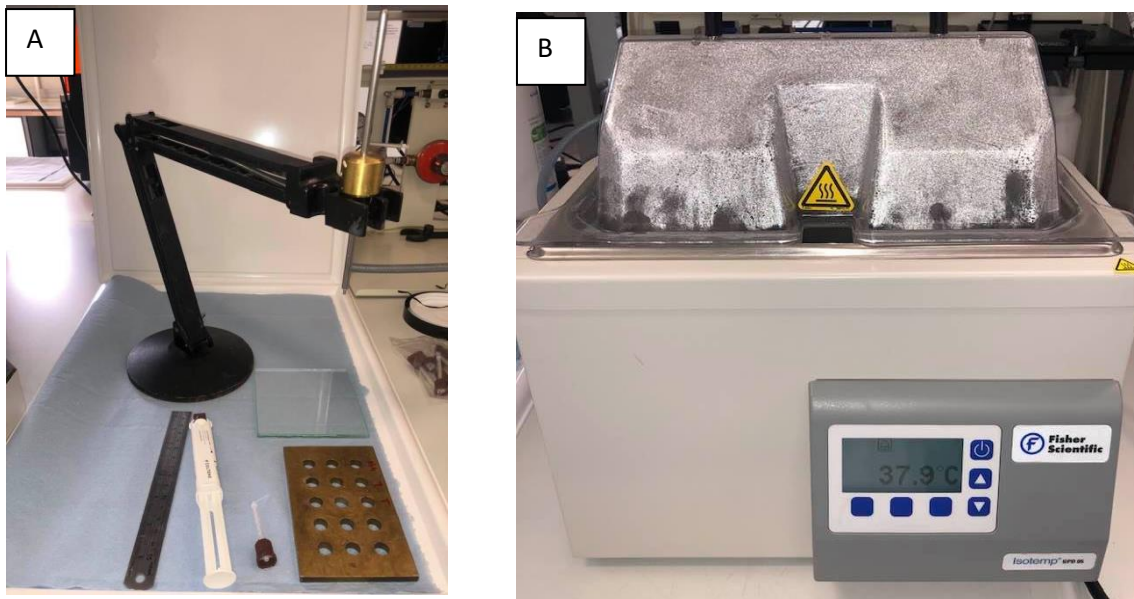


Figure 12 – A) Apparatus required for setting time assessment. B) The water bath was set for 37 °C

9.44 Solubility testing

Discs, (n=3) were prepared for each sealant using circular plastic moulds (10 ± 0.1 mm diameter and 1.0 ± 0.1 mm thickness). The discs were then weighed to determine initial mass and then immersed in distilled water at 37 °C for 24 hours, (Figure 13). The excess water was removed with moistened filter paper. Finally, the samples were dried in an oven until the weight was stable and the final dry mass noted.

Solubility was calculated using the following equation:

Solubility = [(initial mass – final dry mass) / final dry mass] X 100.



Figure 13 – Discs immersed in distilled water for 24 hours

9.5 Ion release and characterisation of the novel sealant and GuttaFlow

Bioseal® discs after immersion in SBF and TBS

Disc specimens (n=84), were prepared using circular plastic moulds (10 ± 0.1 mm diameter and 1.0 ± 0.1 mm thickness).

9.51 IMMERSION MEDIA WERE PREPARED AS FOLLOWS:

9.512 Tris buffer solution

TBS was made by adding 121.14 g of Tris base (hydroxymethyl)aminomethane (Sigma–Aldrich) in 800 ml of distilled water. The solution was then adjusted to pH 7.48 using hydrochloric acid. Further distilled water was then added until the volume reached 1 litre (Mneimne *et al.*, 2011). The prepared solution was preserved in a plastic bottle with a lid and placed in a refrigerator.

9.513 Simulated body fluid

SBF was prepared according to the protocol of Kokubo (Kokubo & Takadama, 2006). 1000 ml of SBF was prepared. Initially, 700 ml of ion-exchanged distilled water was added to a plastic beaker with a magnetic stirring bar and placed over a magnetic heater set to 36.5 °C. The following reagents were then added individually in the following order: sodium chloride (Sigma-Aldrich), sodium hydrogen carbonate (VWR Chemicals), potassium chloride (Sigma-Aldrich), di-potassium hydrogen phosphate trihydrate (VWR Chemicals), magnesium chloride hexahydrate (Sigma-Aldrich), calcium chloride (Sigma-Aldrich), sodium sulfate (Sigma-Aldrich), tris-hydroxymethyl aminomethane (Sigma-Aldrich). Tris and hydrochloric acid were added next carefully until a pH of 7.40 is reached. The prepared solution was preserved in a plastic bottle with a lid and placed in a refrigerator.

9.52 Immersion media investigations

For the immersion investigations, each sealant disc for each predetermined time interval was immersed in 20 ml of SBF and TBS, as prepared above. The tubes had a conical base to ensure the sealant had maximum surface contact with the immersion solution (Figure 14). Discs from each sealant (novel sealant and GFBS (n=3)) were immersed for the following time periods: 1, 7, 14, 21, 28, 44, 77, 84 days.

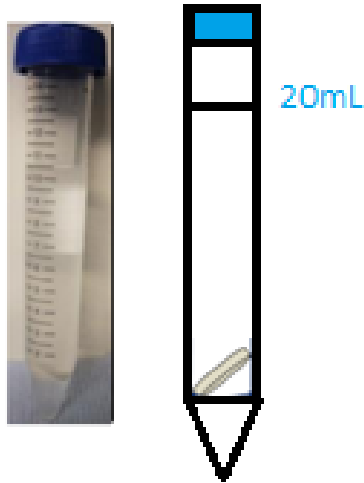


Figure 14 – Sealant placed in a plastic tube with a conical base. Note, the sealant disc was not placed flat on the tube. This was essential to maximise contact with the immersion solution

9.521 pH analysis

The pH meter (Oakton Instruments, Nijkerk, the Netherlands) was calibrated using three standard solutions of pH 4, 7 and 10 prior to sample investigation. At the end of each time point and immediately after the samples were taken out from the shaking incubator, the disc was removed from the immersion solution and the pH measured for each disc, in both SBF and TBS, at every time interval, (Figure 15).

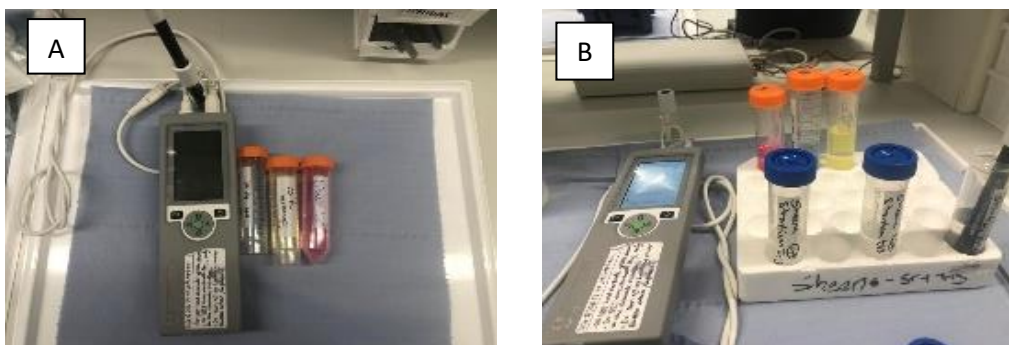


Figure 15 - A) pH measurement apparatus illustrating the pH calibrating solutions (acid, base and neutral solutions) and the pH measurement device. B) pH measurement of novel strontium sealant after immersion in TBS

9.522 Inductively coupled plasma optical emission spectroscopy analysis (ICP-OES)

Inductively coupled plasma optical emission spectroscopy (ICP-OES) analysis ICP-OES (Varian Vista-PRO, Varian Ltd., Oxford, UK) was used to detect the concentrations of phosphorus, calcium, sodium, strontium and silicone from both sealant discs immersed in TBS and SBF solution. The SBF solution used was diluted by a factor of 4 using a combination of water and nitric acid solution (9:1 water:nitric acid ratio). Using this same solution, TBS was diluted by a factor of 2. The purpose of the dilutions was to allow the ion concentration detection to be within the accepted ranges in the ICP-OES machine.

Method:

The immersion solutions were analysed in a machine (Thermo Scientific iCAP 7000 Series ICP spectrometer), (Figure 16). When plasma energy is given to the samples, the component elements (atoms) are excited. These then return to a low energy position and emission rays are released. These correspond to the photon wavelength and are measured. The element type is determined by the position of the photon ray and the content is based on the intensity of the rays.

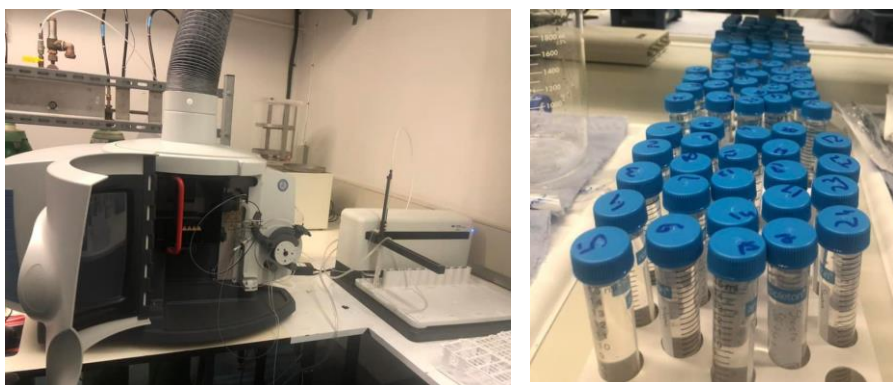


Figure 16 – ICP-OES analysis for the detection of ion release from the endodontic sealants

9.523 Fourier transform infrared spectroscopy (FTIR) analysis

FTIR analysis was performed using Spectrum GX (Perkin-Elmer, Waltham, MA, USA) in the Attenuated Total Reflection (ATR) mode, (Figure 17). The immersed discs, after each time interval were pressed against the FTIR lens to attain maximum signal intensity. Data readings were collected from 1800 to 500 cm^{-1} in absorbance mode for all discs for both sealants at each time interval. They were compared with baseline readings for non-immersed discs and that of hydroxyapatite to assess for apatite formation. The FTIR spectroscopy measures the vibration in the molecular structure of a material. The infrared radiation leads to the vibration and rotation of molecules within the sealant discs when it absorbs the radiation. The energy peak produced corresponds to the frequency of a particular bond. This helps us identify if apatite has formed.



Figure 17 – FTIR analysis using the Spectrum GX (Perkin-Elmer, Waltham, MA, USA)

9.524 X-ray diffraction analysis

X-ray diffraction (XRD) analysis was performed using An X'pert Pro Diffractometer (Panalytical, Netherlands) with Cu-K α alpha radiation. The XRD analysis is reliant on the interaction between the x-ray waves and the crystal lattice structure of a material at an atomic level. It measures the space between the atomic planes. This helps to identify materials and assess if they are crystalline or amorphous in structure. Samples were analysed using a 2θ range of 3-70 degrees, with a step size of 0.03 and a step time of 200 seconds. This was carried out for the discs immersed for 84 days (3 months) for both sealants. The results were compared with baseline readings for non-immersed discs to assess for apatite formation.

9.525 Scanning electron microscopy (SEM) and Energy Dispersive X-ray (EDX) analysis

The three month immersed discs in both SBF and TBS were selected for SEM analysis. The samples were attached to SEM stubs and carbon coated to minimise

charging and improve the image resolution. The image of the sample was taken using the back scatter mode under a 10 KeV beam voltage on scanning electron microscope (FEI Inspect F), along with energy dispersive x-ray detector. Images were taken at a working distance of approximately 10 mm. The SEM is used to assess the surface topography and determine the chemical composition of the material. It works by having an electron beam and rastering it across a sample and detecting secondary or backscattered electron signals. Energy dispersive x-ray (EDX) spectroscopy can then be used to analyse the elemental or chemical characterisation of the sample in the scanned area.

SECTION 10 - RESULTS

Both the novel strontium based endodontic sealant and the GFBS demonstrated physical properties that were in line with the ISO standards. Additionally, they both demonstrated bioactive properties and ion release.

10.1 PHYSICAL PROPERTIES TESTING

10.11 Flow value

The average flow value for GFBS® was 21.25 mm. The average flow value for the novel strontium sealant was 21.17 mm. Both sealants have similar flow values, likely attributed to the fact that they both are embedded within the same matrix and have the same bioactive glass loading dose. Both sealants also met the ISO standards for endodontic sealants which states that each disc shall have a diameter of not less than 17 mm (ISO 6876, 2012), (Table 3, Table 4).

Table 3 – Flow value assessment samples for GFBS

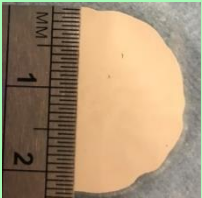



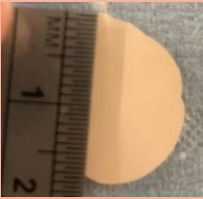





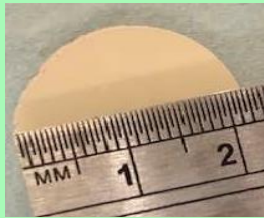
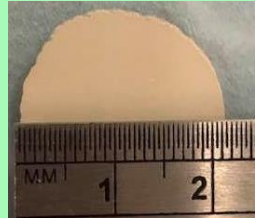
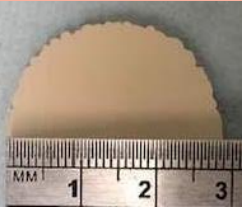
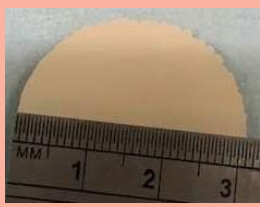

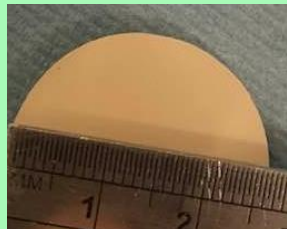
<i>Attempt</i>	<i>GFBS Sample</i>		<i>Accepted / rejected</i>
1	 22 mm	 22 mm	Accepted
2	 20 mm	 19.5 mm	Accepted
3	 18 mm	 22 mm	Rejected
4	 22 mm	 22 mm	Accepted
Average flow value		21.25 mm	
Standard deviation is 1.37			

Table 4 – Flow value assessment samples for the novel strontium sealant

<i>Attempt</i>	<i>Novel strontium sealant Sample</i>		<i>Accepted / rejected</i>
1	 19 mm	 19 mm	Accepted
2	 21.5 mm	 21.5 mm	Accepted
3	 29 mm	 31 mm	Rejected
4	 23 mm	 23 mm	Accepted
Average flow value		21.17 mm	
Standard deviation is 1.73			

10.12 Solubility

Table 5 provides the solubility results obtained for all disc samples for both sealants. The average solubility for the GFBS® was 1.77 %, whilst that for the novel strontium sealant was 0.08 %. The novel strontium sealant demonstrated very little solubility after 24 hours immersion. Both the sealants met ISO standards, which states that the solubility of a sealer shall not exceed 3 % mass fraction after immersion in water for 24 hours (ISO 6876, 2012).

Table 5 – Solubility testing results for the GFBS and novel sealant.

Sealant	Solubility	Average
GuttaFlow Bioseal 1	1.97 %	
GuttaFlow Bioseal 2	1.33 %	
GuttaFlow Bioseal 3	2.01 %	
GuttaFlow Bioseal average		1.77 %
Standard deviation is 0.59		
Novel sealant 1	0.09 %	
Novel sealant 2	0.09 %	
Novel sealant 3	0.05 %	
Novel sealant average		0.08 %
Standard deviation is 0.02		

10.13 Radiopacity

A higher radiopacity value was seen for the novel sealant (5.54 mm/Al) (Table 6) in comparison with the GFBS® (4.08 mm/Al), (Table 7). As the results appeared to show a marked difference in radiopacity between both endodontic sealants, a paired T-test analysis was carried out (Appendix I). The results demonstrated a clear difference, with the novel sealant being significantly more radiopaque than the commercial ($p < 0.05\%$). Both sealants met the ISO standards, which states that the sealant shall have a radiopacity equivalent to not less than 3 mm of a relevant aluminium thickness (ISO 6876, 2012).

Table 6 - Radiopacity values (in mm/Al) for GFBS. Three discs for each sealant has been exposed 6 times.

GFBS SAMPLE	1	2	3
Radiopacity value (mm/Al)	4.09	4.01	3.97
Radiopacity value (mm/Al)	4.57	4.62	4.51
Radiopacity value (mm/Al)	3.99	4.51	4.42
Radiopacity value (mm/Al)	3.90	3.49	4.02
Radiopacity value (mm/Al)	4.43	4.02	4.11
Radiopacity value (mm/Al)	3.52	3.69	3.57
Average mean value			4.08
Standard deviation is 0.33			

Table 7 - Radiopacity values (in mm/Al) for the novel strontium sealant. Three discs for each sealant has been exposed 6 times.

Novel Sr Sealant sample	1	2	3
Radiopacity value (mm/Al)	6.28	6.34	6.30
Radiopacity value (mm/Al)	5.16	5.27	5.32
Radiopacity value (mm/Al)	5.18	5.23	5.63
Radiopacity value (mm/Al)	5.48	5.83	5.37
Radiopacity value (mm/Al)	5.27	5.32	5.97
Radiopacity value (mm/Al)	5.23	5.31	5.29
Average mean value			5.54
Standard deviation is 0.42			

10.14 Setting time reaction

The average setting time for the GFBS[®] was 45.33 minutes, (table 8) whilst that for the novel strontium sealant was 65.00 minutes (table 9). A longer setting time was seen for the novel sealant in comparison with the GFBS[®]. The final setting time for GFBS[®] has not been reported by the manufacturer, however, results from this experiment are similar to a previous one, where a setting time of 45 minutes was reported (Gandolfi *et al.*, 2016). The manufacturer's have reported a curing time for GFBS[®] as 12-16 minutes. However, curing refers to the toughening or hardening of a material, rather than full set. Therefore, the full setting time reported here for GFBS

(45.33 minutes) is much higher than the curing time reported by the manufacturer (12-16 minutes). ISO standards require sealants to have a final setting time to be no more than 10% longer than that claimed by the manufacturer for setting times under 30 mins and for those materials claimed to set between 30 mins up to 72 hours the setting time must be completed within this period (ISO 6876, 2012).

Table 8 - Gutttaflow Bioseal Setting Time Assessment:













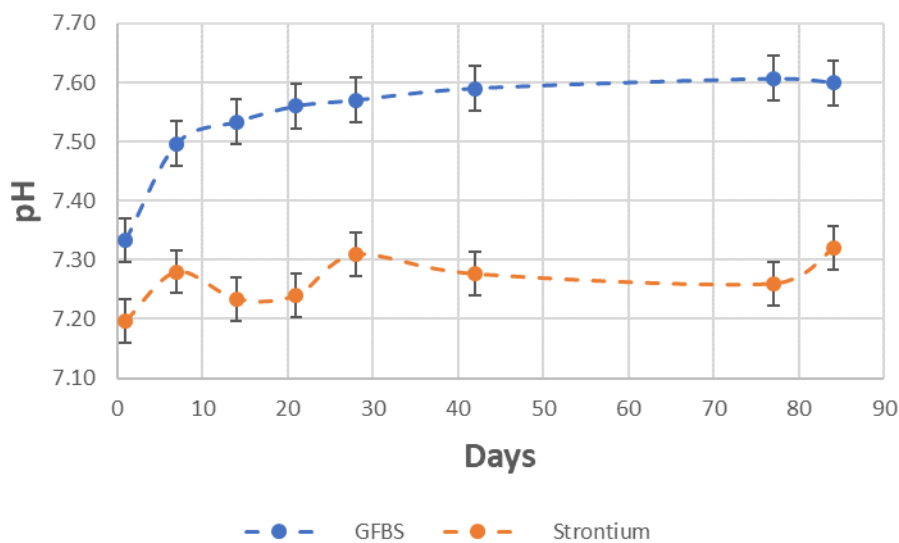
Sample			Setting time
1			43 minutes
2			46 minutes
3			47 minutes
Average setting time			45.33 minutes
Standard deviation is 1.89			

Table 9 - Novel Strontium Sealant Setting Time Assessment:

Sample	Setting time	
1		 <p data-bbox="1034 365 1198 398">57 minutes</p>
2		 <p data-bbox="1034 775 1198 808">68 minutes</p>
3		 <p data-bbox="1034 1178 1198 1211">70 minutes</p>
Average setting time		65 minutes
Standard deviation is 4.95		

10.211 pH changes in SBF solution

A higher pH rise was seen for GFBS than the novel strontium sealant, (Figure 18). The highest pH rise for GFBS was seen at approximately 45 days, after which it appears to be maintained for 3 months. The highest pH rise for the novel strontium sealant appears to be just after 25 days, and gradually reduces after 40 days. Interestingly, there is a steep increase in pH at the 3-month mark.



*Error bars have been included to visualise variability of the plotted data

Figure 18 – pH changes in SBF solution for GFBS and the novel sealant

10.212 pH changes in Tris buffer solution

A higher pH rise was seen for GFBS than the novel strontium sealant, (Figure 19). Both sealants appear to have a decline in the pH at approximately 14 days and then an increase at approximately 20 days. The highest pH rise for both sealants appeared to occur after approximately 25 days, after which a small dip was seen. GFBS appears

to maintain its high pH for a prolonged period, however, the pH appears to slightly decline for the novel strontium-based sealant.

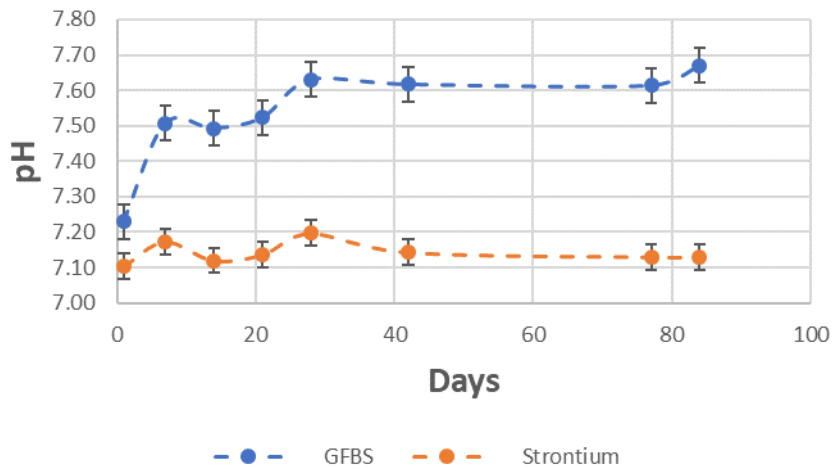
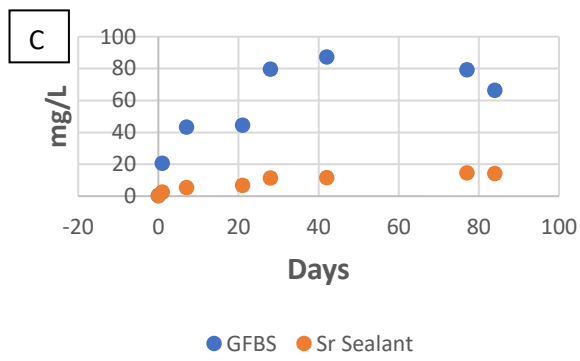
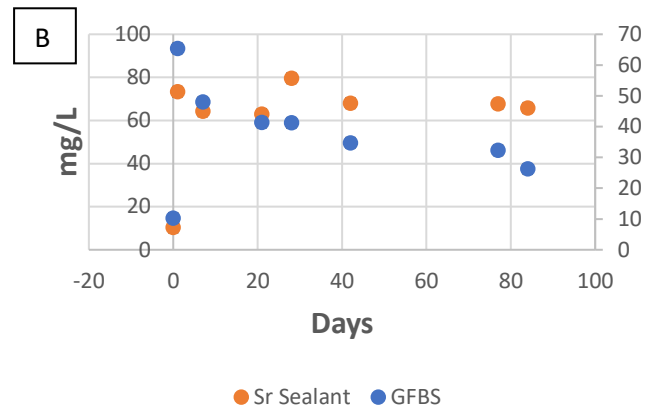
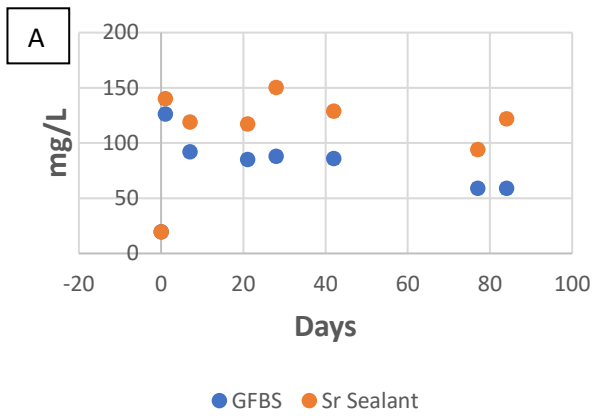


Figure 19 – pH changes in TBS for GFBS and the novel sealant

10.22 Ion release Profiles

Both sealants demonstrated release of ions, which, not surprisingly, comprised the contents of the bioactive glass. A higher calcium and phosphate ion release was seen from the novel sealant in SBF, (Figure 20). By comparison, a higher ion release was seen in TBS from GFBS®, (Figure 21). The novel sealant demonstrated additional release of strontium ions, (Figure 22).

From the assessed data, Na⁺ ion release appears to have a square root time dependence. (Figure 23). There was only a small amount of sodium release from the novel sealant in TBS and SBF.



*Error bars have been included, arising from the ICP-OES analysis measurements only

Figure 20 – A) Ca ion release in SBF, B) P ion release in SBF, C) Si ion release in SBF

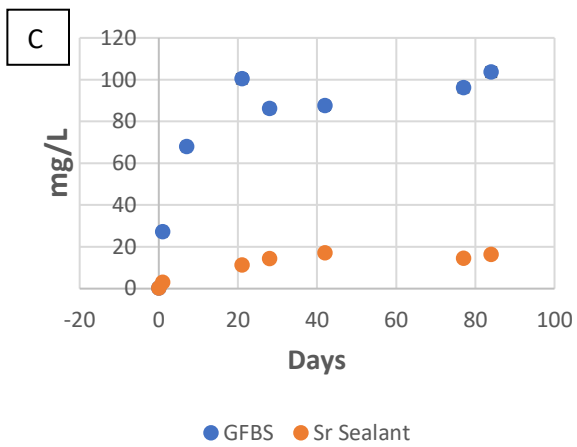
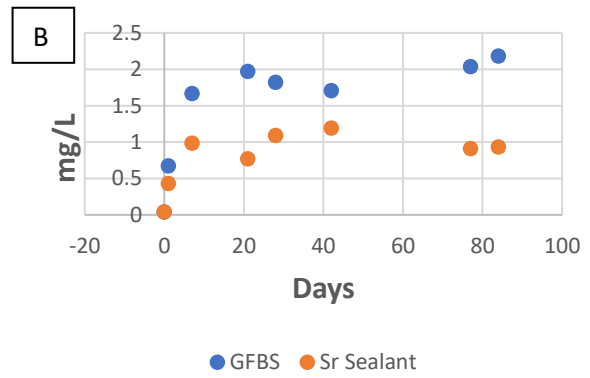
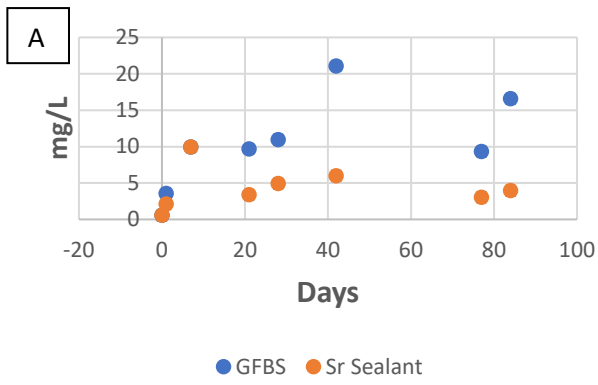


Figure 21 – A) Ca Ion release in TBS, B) P Ion release in TBS, C) Si Ion release in TBS

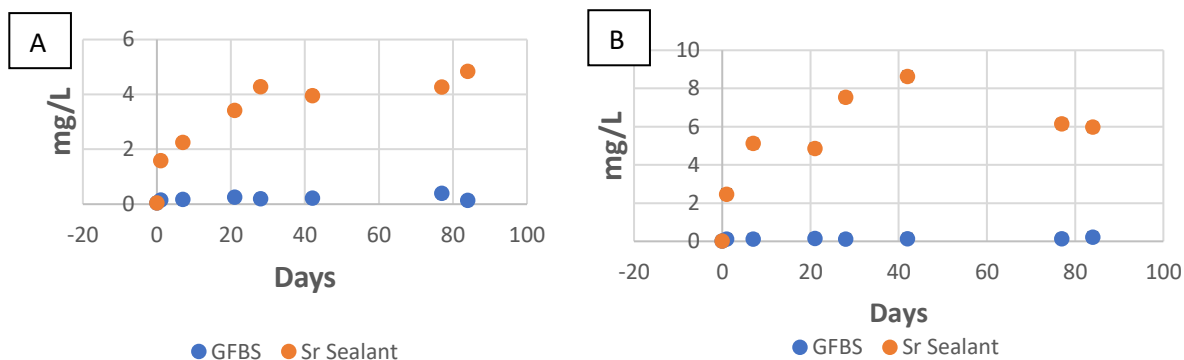


Figure 22 – Sr ion release in A) SBF and B) TBS

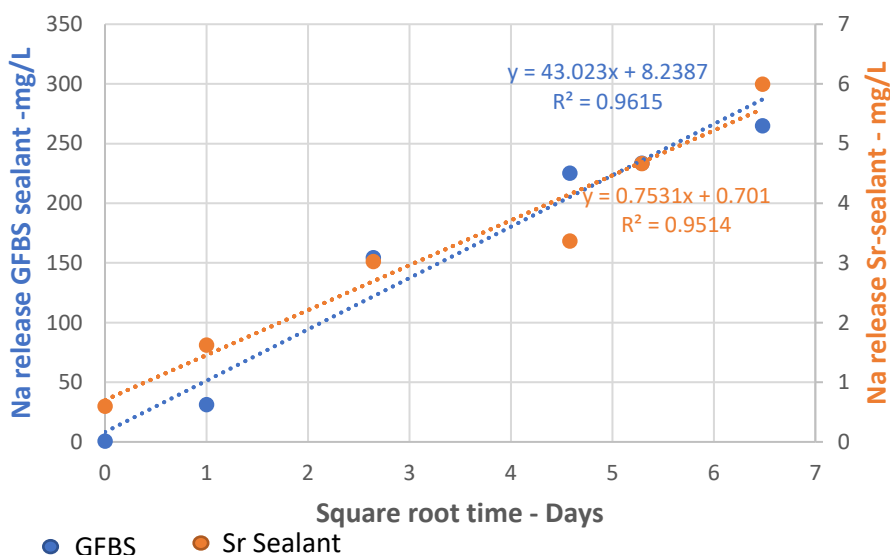


Figure 23 – Na Ion release in TBS analysis against square root time

10.23 Apatite formation

X-Ray Diffraction patterns at the three-month immersion period show weak intensities for apatite formation in GFBS® immersed in SBF, (Figure 24). There is no clear evidence of apatite formation from the novel strontium-based sealant, (Figure 25).

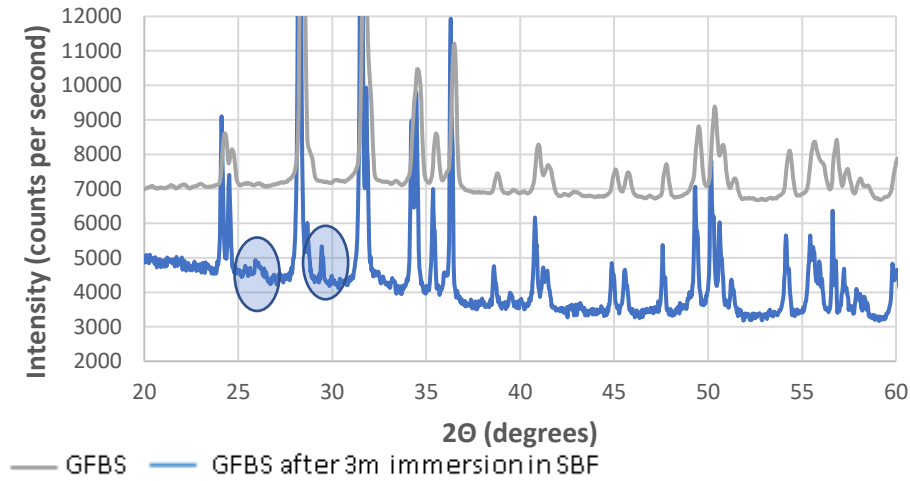


Figure 24 – XRD analysis of GFBS after a 3-month immersion period in SBF. The highlighted areas demonstrate weak intensities for apatite formation.

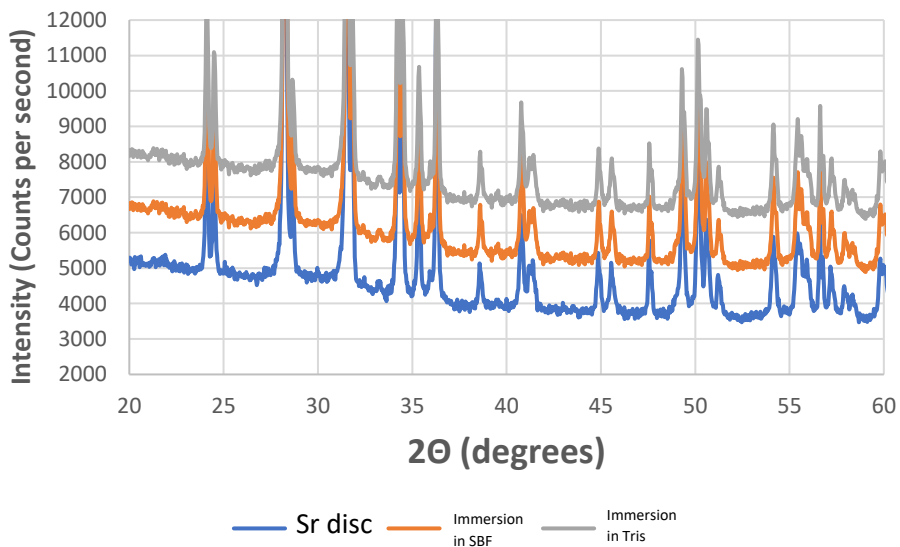


Figure 25 – XRD analysis of the novel sealant after a 3-month immersion period in SBF and TBS

SECTION 11 - DISCUSSION

11.1 DISCUSSION OF RESULTS WITH COMPARISON TO PREVIOUS STUDIES

The addition of bioactive glass fillers in endodontic sealants is aimed at promoting apical healing by the dissolution of the glass particles and subsequent ability to form apatite, aid bone regeneration and improve the sealing capacity of the root filling.

The results from this study are in line with previous literature where GFBS[®] was shown to release ions and form apatite in SBF (Hoikkala *et al.*, 2018). The weak diffraction lines from XRD analysis at the three-month immersion period in SBF (at 26.1 2 θ and 33-34 2 θ) are indicative of an apatite formation (Figure 24). The interferences from the zirconia filler, added to provide radiopacity, makes the accurate analysis of apatite formation challenging. In contrast there is no clear evidence of apatite formation in TBS. This is possibly because SBF is saturated with Ca²⁺ and PO₄³⁻ ions and therefore it is easier to form apatite. Clinically, the ability to form bone-like carbonated apatite can aid in regeneration of bony defects seen in long-standing endodontic infections (Väkiparta *et al.*, 2005). Previous studies have shown that when bioactive glass is implanted into a bony defect, it bonds directly to the bone via an apatite layer, without the intervention of connective tissues (Kokubo & Yamaguchi, 2019). No clear evidence of apatite formation was seen in the novel strontium-based endodontic sealant either in TBS or SBF. A possible reason for this may be because the bioactive glass used in this sealant has a higher network connectivity (network connectivity – 2.28), therefore making it more cross-linked and less soluble in comparison with the 45S5 bioactive glass (network connectivity – 2.11). Therefore, it takes a longer time to degrade. We can tell from the results of the pilot study (where the novel strontium bioactive glass

was immersed in SBF and TBS, that apatite was shown to form within 7 days), that the novel sealant is bioactive and can form apatite. A longer study could possibly show apatite formation from the novel sealant.

The mechanism of action for bioactive glasses is thought to arise from the cation exchange from the glass ion modifiers Na^+ and Ca^{2+} and H_3O^+ or H^+ ions from body fluid. There is then a breakdown of Si-O-Si bonds at the glass/solution interface. This forms a poorly connected silica rich layer. Then, amorphous calcium hydroxyl phosphate precipitates on the silica rich layer (calcium ions precipitation followed by incorporation of the $\text{OH}/\text{PO}_4^{3-}$ anions from the supersaturated solution). This crystallises to form a hydroxycarbonate apatite which can bond to bone or tooth (Hench, 2006), (Washio *et al.*, 2019). As expected, the novel strontium-based sealant released higher Ca^{2+} and PO_4^{3-} ions in SBF compared with GFBS. This can be explained by the significantly higher PO_4^{3-} content in the glass; with the novel sealant containing over 2.5x more PO_4^{3-} content. In general, there was less ion release across all elements in TBS, from the novel strontium-based sealant. This maybe because the novel strontium-based sealant is less soluble as a result of its higher network connectivity and Na_2O content. This is particularly noticeable for sodium ion release. Sodium salts are very soluble and there was a much higher ion release from the GFBS immersed in tris than the novel strontium-based sealant - by over 50 times. Ion release can be improved by increasing the bioactive glass content in the sealant, or alternatively, lowering the network connectivity of the glass, thus making the glass more degradable.

The novel sealant demonstrates improved physical properties with virtually no solubility and improved radiopacity. Assessing the solubility of sealants is important as an insoluble sealant can help to prevent apical leakage and improve seal. From the

physical tests analysis, we can see that the solubility of GFBS is over 20 times higher than that of the novel sealant. A likely explanation for this may be seen from the sodium ion release data; sodium ions have a diffusion rate dependence, (Figure 23), and sodium salts do not precipitate (unlike Ca^{2+} and PO_4^{3-}). Therefore, assessing Na^+ ion release can help assess the degradation and solubility of a material. A linear regression equation was calculated for sodium ion release against square root time and had a correlation coefficient close to 1 (0.9615 for GFBS and 0.9514 for the novel strontium sealant). The gradient of the Na^+ ion release from GFBS was 50 times greater than that of the novel sealant. This explains why the solubility was higher from the GFBS than from the novel sealant. It is important to acknowledge, that whilst both sealants meet the ISO standards for solubility, the data from this study shows a continuous ion release profile over a 3-month period. This means that as further ions are released, the solubility of the material increases over time and can have a significant impact on the sealing properties of the sealant. The GFBS could exceed a solubility range of 3% over a period of 3 months as the material's solubility already reached 1.77% after just 24 hours immersion. Given these findings, solubility tests should perhaps be evaluated for longer periods to correlate with clinical conditions.

The addition of strontium to the bioactive glass has promising results in current research. From this study, we can see that the addition of strontium can help to confer radiopacity to the sealant because of its high atomic number. The radiopacity from the novel sealant is almost double (1.85x) that required by the ISO standard. Zirconia is added in the commercial GFBS to confer radiopacity. As strontium helps with the radiopacity of an endodontic sealant, a novel sealant can be created minimising the amount of zirconia filler content, whilst adding more bioactive glass, without

compromising on viscosity of the sealant. As well as maintaining the radiopacity, this will also clearly improve the bioactive properties of the sealant.

The substitution of strontium for calcium ions in the novel sealant has been shown to have a further favourable impact on bone cells. They are currently being used in other medical applications, such as the treatment of osteoporosis (Dahl *et al.*, 2001). A study conducted by Gentlemen *et al.*, showed that strontium-substituted bioglass promotes osteoblast proliferation and reduces the osteoclast activity in cell culture (Gentleman *et al.*, 2010). It is thought that cells respond better to strontium ions in solution for bone regeneration. From this study, we can see a constant release of strontium ions into SBF solution (with no clear evidence of precipitation). Clinically, the continuous ion release could aid in regenerating large bony defects, as seen in long standing apical periodontitis. This may help improve the prognosis for such lesions. The release of ions, and the rate of release of ions from this study show very similar results to a similar study conducted by Hoikkala in 2018. Their experiments tested ion-release by ICP-OES in a similar fashion (unlike other similar studies which use ethylene diamine tetraacetic acid (EDTA) titration method). What was interesting in the Hoikkala study was that when the GFBS was grounded (thus the particle size was reduced), the rate and amount of calcium and phosphate ion release was increased (Hoikkala *et al.*, 2018). This demonstrates that particle size has an important role in biomineralisation, and that small particle size can perform better in inducing biomineralisation.

Both sealants showed a rise in pH values. The pH rise was greater in the GFBS than the novel strontium-based sealant on both immersion solutions (SBF and Tris). This again is likely to be due to the higher Na⁺ content and lower network connectivity of the GFBS. From Hench's earlier literature, the first stage in glass degradation is Na⁺ ion exchange for H⁺ which creates the increase in pH. Therefore, a higher Na⁺ content

in 45S5 will cause a faster and more pronounced alkaline pH rise. It has been shown that a pH rise in endodontic sealant can confer antimicrobial effects, and stimulate the deposition of mineralised tissue (by activating the calcium dependent adenosine triphosphatase), which, in turn, can aid healing. In addition, the increase in pH can help to neutralise lactic acid produced by osteoclasts (therefore preventing the dissolution of mineralised components) (Okabe *et al.*, 2006). An alkaline pH can also encourage a prolonged setting time and a long-lasting antibacterial effect that eliminates residual microorganisms surviving along dentinal walls (Silva *et al.*, 2013). This may lead to eradication of persistent bacteria which survived the chemo-mechanical procedure during root canal treatment. The novel sealant clearly demonstrated a rise in pH with a steep increase in the 3-month period, (Figure 18). Unlike the commercial sealant, which appears to be plateauing at 3-month immersion in SBF, the pH of the novel sealant continues to increase, demonstrating a long-term benefit from this rise in pH.

11.2 LIMITATIONS OF THE STUDY

A limitation of this study was that the experiments were conducted in-vitro, as a first step. Unlike the media used in the experiments (SBF and Tris), endodontic sealants are exposed to real body fluids (interstitial tissue fluids from the dental pulp or periodontal ligament). Such fluids have been shown to contain various proteins, such as albumin. Albumin has been shown to inhibit apatite formation by obstructing apatite nucleation sites (D'Elia *et al.*, 2017). Therefore, future research into bioactive endodontic sealants should include clinical trials with appropriate ethical approval to demonstrate real clinical effects of bioactive strontium-based endodontic sealants.

SECTION 12.1 - CONCLUSION

Bioactive glasses have been recently introduced into the dental materials and have consistently shown to have promising effects. Altering the composition of the bioactive glass can target an optimal endodontic sealant formula. The addition of strontium into sealants shows promising effects in *in-vitro* tests.

Whilst both the novel strontium sealant and the commercial GFBS show physical properties in line with the ISO standards, the novel sealant demonstrates enhanced physical properties. The novel sealant has virtually no solubility ((0.08 %), which is 22 times less soluble than the GFBS) and it has excellent radiopacity due to the presence of high atomic strontium ions. As expected, the flow values and setting time are similar for both sealants; likely attributed to the fact that they are both composed of the same PDMS matrix and undergo similar chemical setting reactions.

GFBS demonstrates apatite formation after 3-month immersion in SBF. Although apatite formation was not apparent from the novel strontium sealant during the three-month experimental period, ion release (Ca, P and Sr) was clearly demonstrated and therefore the beneficial effects of these ions are present. It can be expected that if the testing was carried out over a longer period of time, apatite formation could be seen from the novel sealant. This is hypothesised as the novel strontium bioactive glass has demonstrated in the pilot study the ability to form apatite after immersion in SBF and TBS after 7 days. This theory is further supported by the fact that there is continuous release of ions from the solution after immersion of the novel strontium sealant in SBF and TBS even at 3-months, with limited evidence of precipitation yet.

As expected, the novel strontium sealant demonstrated additional release of strontium ions in both SBF and TBS. This can have promising effects *in-vivo* such as promoting osteoblast proliferation and aiding bone regeneration.

Further testing can be done to optimise the composition of the novel strontium sealant. The bioactivity of the sealant can be enhanced by increasing the loading percentage of glass in the matrix, or alternatively by lowering the network connectivity of the glass; which allows the glass to degrade faster and therefore result in further ion release.

SECTION 12.2 - RECOMMENDATIONS

The data shown in this research showed positive benefits from the addition of strontium into a novel bioactive endodontic sealant. Given the promising results obtained, there is further scope for advanced research based on these current findings.

It would be interesting if the further studies are performed on a physical and biological basis, both *in vitro* and *in vivo*:

1 – Physical testing

Since it is claimed that this novel strontium based endodontic sealant is to be used in endodontic obturation, the sealing ability of the novel sealant should be assessed. This can be done by assessment of leakage measurements (for example with the use of a subnanoliterscaled fluid measuring device or using dye or bacterial penetration tests and sectioning roots). The results from this can be compared with current commercial sealants such as GFBS[®] and Tubliseal[®].

2 – Biocompatibility and antimicrobial effects

A – Cell culturing

The effects of cell viability can be assessed *in vitro* using cementoblast or osteoblast like cells, with alkaline phosphatase (ALP) enzyme activity to assess cell differentiation.

B – Bacterial adhesion

The bacterial adhesion to the novel strontium endodontic sealant can be examined to assess the antimicrobial effects of the novel sealant.

3 – Clinical assessment

The applicability of the novel strontium based endodontic sealant needs to be explored *in-vivo*. This can be done using long-term success/survival studies.

SECTION 13 - REFERENCES

1. Ali A, Sümbüllü M, İshaq A, Arslan H. Localized contact urticaria due to epoxy resin-based endodontic sealer. *Saudi Endod J*, 2022; 12:222-6
2. Bagchi, A, Meka, S, Rao, B. and Chatterjee, K, Perovskite. Ceramic nanoparticles in polymer composites for augmenting bone tissue regeneration. *Nanotechnology*, 2014; 25(48), p.485101.
3. Barbizam JV, Souza M, Cecchin D, Dabbel J. Effectiveness of a silicon-based root canal sealer for filling of simulated lateral canals. *Braz Dent J*. 2007;18(1):20-3. doi: 10.1590/s0103-64402007000100005. PMID: 17639195.
4. Brauer D, Karpukhina N, Law R, Hill R. Structure of fluoride containing bioactive glasses. *J Mater Chem*, 2009;19;5629-36.
5. Camargo RV, Silva-Sousa YTC, Rosa RPF, et al. Evaluation of the physicochemical properties of silicone- and epoxy resinbased root canal sealers. *Braz Oral Res*, 2017;31:e72.
6. Camilleri J. Characterization and hydration kinetics of tricalcium silicate cement for use as a dental biomaterial. *Dent Mater*. 2011 Aug;27(8):836-44. doi: 10.1016/j.dental.2011.04.010. Epub 2011 May 19. PMID: 21600643.
7. Camps J, Jeanneau C, El Ayachi, Laurent P. and About I. Bioactivity of a Calcium Silicate–based Endodontic Cement (BioRoot RCS): Interactions with Human Periodontal Ligament Cells In Vitro. *Journal of Endodontics*, 2015, 41(9), pp.1469-1473.
8. Cannio M. “Bioactive glass applications: A literature review of Human Clinical Trials,” *Materials*, 2021, 14(18), p. 5440. Available at: <https://doi.org/10.3390/ma14185440>.

9. Collado-Gonzalez M, Tomas-Catala CJ, Onate-Sanchez RE, Moraleda JM, Rodriguez-Lozano FJ. Cytotoxicity of GuttaFlow Bioseal, GuttaFlow2, MTA Fillapex, and AH Plus on human periodontal ligament stem cells. *J Endod*, 2017; 43:816–22.
10. D Ricucci, I Rôças, F Alves, S Loghin, and J. F. Siqueira, “Apically extruded sealers: fate and influence on treatment outcome,” *Journal of Endodontics*, 2016; 42(2), pp. 243–249.
11. Dahl S, Allain P, Marie P, Mauras Y, Boivin G, Ammann P, Tsouderos Y, Delmas P. and Christiansen C. Incorporation and distribution of strontium in bone. *Bone*, 2001, 28(4), pp.446-453.
12. D'Elia N, Gravina N, Ruso J, Marco-Brown J, Sieben J and Messina P. Albumin-mediated deposition of bone-like apatite onto nano-sized surfaces: Effect of surface reactivity and interfacial hydration. *Journal of Colloid and Interface Science*, 2017, 494, pp.345-354.
13. DeLong C, He J, Woodmansey KF. The effect of obturation technique on the push-out bond strength of calcium silicate sealers. *J Endod*. 2015 Mar;41(3):385-8. doi: 10.1016/j.joen.2014.11.002. Epub 2015 Jan 6. PMID: 25576202.
14. Dentistry — Root canal sealing materials., 2012. International Standards Organisation (ISO) 1-9.
15. Desai S. and Chandler N, Calcium Hydroxide–Based Root Canal Sealers: A Review. *Journal of Endodontics*, 2009, 35(4), pp.475-480.
16. Deshmukh K, Kovarik T, Krenek T, Docheva D, “Recent advances and future perspectives of sol–gel derived porous bioactive glasses: A Review,” *RSC*

Advances, 2020, 10(56), pp. 33782–33835. Available at: <https://doi.org/10.1039/d0ra04287k>.

17. Dunfee BL, Sakai O, Pistey R, Gohel A, Radiologic and pathologic characteristics of benign and malignant lesions of the mandible. *Radiographics*, 2006, 26:1751–1768
18. Edén M. “The split network analysis for exploring composition–structure correlations in multi-component glasses: I. Rationalizing bioactivity-composition trends of bioglasses,” *Journal of Non-Crystalline Solids*, 2011, 357(6), pp. 1595–1602. Available at: <https://doi.org/10.1016/j.jnoncrysol.2010.11.098>.
19. G Bardini, L Casula, E Ambu, D Musu, M Mercadè, and E Cotti, “A 12-month follow-up of primary and secondary root canal treatment in teeth obturated with a hydraulic sealer,” *Clinical Oral Investigations*, 2021, 25(4), pp. 2757–2764, 2021.
20. Gambarini G. and Tagger M. “Sealing ability of a new hydroxyapatite-containing endodontic sealer using lateral condensation and thermatic compaction of gutta-percha, in vitro,” *Journal of Endodontics*, 1996, 22(4), pp. 165–167.
21. Gandolfi M., Siboni F. and Prati C, Properties of a novel polysiloxane-guttapercha calcium silicate-bioglass-containing root canal sealer. *Dental Materials*, 2016; 32(5), pp.e113-e126.
22. Gee A.J, WU K, and Wesselink P.R. Sealing properties of KETAC-endo glass ionomer cement and AH26 root canal sealers. *International Endodontic Journal*, 1994; 27(5), pp. 239–244. Available at: <https://doi.org/10.1111/j.1365-2591.1994.tb00262.x>.
23. Geethapriya N, Subbiya A, Mitthra S, Prakash V. Accidental Large Extrusion of Epoxy Resin Sealer in the Periapical Area-A Case Report with three Years

- Follow up. Indian Journal of Public Health Research & Development. 2019;10(8):1610-4.
24. Gentleman E, Fredholm Y, Jell G, Lotfibakhshaiesh N, O'Donnell M, Hill R and Stevens M. The effects of strontium-substituted bioactive glasses on osteoblasts and osteoclasts in vitro. *Biomaterials*, 2010, 31(14), pp.3949-3956.
25. Gomes BPFA, and Herrera DR. Etiologic role of root canal infection in apical periodontitis and its relationship with clinical symptomatology. *Braz Oral Res*. 2018 Oct 18;32(suppl 1):e69. doi: 10.1590/1807-3107bor-2018.vol32.0069. PMID: 30365610.
26. Han X. et al. "Novel bioactive glass-modified hybrid composite resin: Mechanical properties, biocompatibility, and antibacterial and remineralizing activity," *Frontiers in Bioengineering and Biotechnology*, 2021, 9. Available at: <https://doi.org/10.3389/fbioe.2021.661734>.
27. Hench L, Splinter R, Allen W, and Greenlee T. Bonding mechanisms at the interface of ceramic prosthetic materials. *Journal of Biomedical Materials Research*, 1971, 5(6), pp.117-141.
28. Hill R.G. and Brauer D.S. "Predicting the bioactivity of glasses using the network connectivity or split network models," *Journal of Non-Crystalline Solids*, 2011, 357(24), pp. 3884–3887. Available at: <https://doi.org/10.1016/j.jnoncrysol.2011.07.025>.
29. Hoikkala N, Siekkinen M, Hupa L. and Vallittu P. Behaviour of different bioactive glasses incorporated in polydimethylsiloxane endodontic sealer. *Dental Materials*, 2021, 37(2), pp.321-327.
30. Hoikkala N, Wang X, Hupa L, Smatt J, Peltonen J and Vallittu, P. Dissolution and mineralization characterization of bioactive glass ceramic containing

- endodontic sealer Guttaflow Bioseal. *Dental Materials Journal*, 2018, 37(6), pp.988-994.
31. Holland R, Filho J, Cintra L, Esterla C, “Factors affecting the periapical healing process of endodontically treated teeth,” *Journal of Applied Oral Science*, 2017, 25(5), pp. 465–476. Available at: <https://doi.org/10.1590/1678-7757-2016-0464>.
32. Huang F.-M, Tai K-W, Chou M-Y, Chang Y.C. “Cytotoxicity of resin-, zinc oxide-eugenol-, and calcium hydroxide-based root canal sealers on human periodontal ligament cells and permanent V79 cells,” *International Endodontic Journal*, 2002, 35(2), pp. 153–158. Available at: <https://doi.org/10.1046/j.1365-2591.2002.00459.x>.
33. Huang, M., Hill, R. and Rawlinson, S. Strontium (Sr) elicits odontogenic differentiation of human dental pulp stem cells (hDPSCs): A therapeutic role for Sr in dentine repair? *Acta Biomaterialia*, 2016, 38, pp.201-211.
34. Jung S, Sielker S, Hanisch MR, Libricht V, Schäfer E, Dammaschke T. Cytotoxic effects of four different root canal sealers on human osteoblasts. *PLoS One*. 2018; 13(3):e0194467. doi: 10.1371/journal.pone.0194467. PMID: 29579090; PMCID: PMC5868789.
35. Kakehashi, S, Stanley, H.R. and Fitzgerald, R.J. “The effects of surgical exposures of dental pulps in germ-free and conventional laboratory rats,” *Oral Surgery, Oral Medicine, Oral Pathology*, 20(3), 1965, pp. 340–349. Available at: [https://doi.org/10.1016/0030-4220\(65\)90166-0](https://doi.org/10.1016/0030-4220(65)90166-0).
36. Kakehashi S, Stanley H.R. and Fitzgerald, R.J. “The effects of surgical exposures of dental pulps in germ-free and conventional laboratory rats,” *Oral*

- Surgery, Oral Medicine, Oral Pathology, 1965, 20(3), pp. 340–349. Available at: [https://doi.org/10.1016/0030-4220\(65\)90166-0](https://doi.org/10.1016/0030-4220(65)90166-0).
37. Kaur G, Pickrell G, Sriranganathan, N, Kumar V, and Homa D. “Review and the State of the art: Sol–gel and melt quenched bioactive glasses for tissue engineering,” *Journal of Biomedical Materials Research Part B: Applied Biomaterials*, 2015, 104(6), pp. 1248–1275. Available at: <https://doi.org/10.1002/jbm.b.33443>.
38. Keleş A, Köseoğlu M. Dissolution of root canal sealers in EDTA and NaOCl solutions. *J Am Dent Assoc.* 2009; 140(1):74-9; quiz 113. doi: 10.14219/jada.archive.2009.0021. PMID: 19119170.
39. Khandelwal A, Janani K, Teja K, Jose J, Battineni G, Riccitiello F, Valletta A, Palanivelu A, Spagnuolo G. Periapical Healing following Root Canal Treatment Using Different Endodontic Sealers: A Systematic Review. *Biomed Res Int.* 2022; 2022:3569281. doi: 10.1155/2022/3569281. PMID: 35845966; PMCID: PMC9286882.
40. Kim YK, Grandini S, Ames JM, Gu LS, Kim SK, Pashley DH, Gutmann JL, Tay FR. Critical review on methacrylate resin-based root canal sealers. *J Endod.* 2010; 36(3):383-99. doi: 10.1016/j.joen.2009.10.023. PMID: 20171352.
41. Koh, E.T. “Cellular response to mineral trioxide aggregate,” *Journal of Endodontics*, 1998, 24(8), pp. 543–547. Available at: [https://doi.org/10.1016/s0099-2399\(98\)80074-5](https://doi.org/10.1016/s0099-2399(98)80074-5).
42. Kokubo, T. and Takadama, H. How useful is SBF in predicting in vivo bone bioactivity? *Biomaterials*, 2006, 27(15), pp.2907-2915.

43. Kokubo, T and Yamaguchi S. Simulated body fluid and the novel bioactive materials derived from it. *Journal of Biomedical Materials Research Part A*, 2019, 107(5), pp.968-977.
44. Komabayashi, T. et al. "Comprehensive review of current endodontic sealers," *Dental Materials Journal*, 2020, 39(5), pp. 703–720. Available at: <https://doi.org/10.4012/dmj.2019-288>.
45. Le Pevelen, D.D. "X-ray crystallography of small molecules: Theory and workflow," *Encyclopedia of Spectroscopy and Spectrometry*, 2017, pp. 624–639. Available at: <https://doi.org/10.1016/b978-0-12-409547-2.05260-4>.
46. Li Y, Chen L, Chen X, Hill R, Zou S, Wang M, Liu Y, Wang J, and Chen, X, High phosphate content in bioactive glasses promotes osteogenesis in vitro and in vivo. *Dental Materials*, 2021, 37(2), pp.272-283.
47. Liu J, Rawlinson S, Hill R. and Fortune F. Strontium-substituted bioactive glasses in vitro osteogenic and antibacterial effects. *Dental Materials*, 2016, 32(3), pp.412-422.
48. Lyu W.-J. et al. "Physicochemical properties of a novel bioceramic silicone-based root canal sealer," *Journal of Dental Sciences*, 2022, 17(2), pp. 831–835. Available at: <https://doi.org/10.1016/j.jds.2021.09.034>.
49. M Bernáth and J Szabó, "Tissue reaction initiated by different sealers," *International Endodontic Journal*, 2003, 36(4), pp. 256–261.
50. Marsh P.D. "Are dental diseases examples of ecological catastrophes?," *Microbiology*, 2003, 149(2), pp. 279–294. Available at: <https://doi.org/10.1099/mic.0.26082-0>.

51. Mohammadi Z, Dummer PM. Properties and applications of calcium hydroxide in endodontics and dental traumatology. *Int Endod J.* 2011 Aug;44(8):697-730. doi: 10.1111/j.1365-2591.2011.01886.x. Epub 2011 May 2. PMID: 21535021.
52. Moller, Å.K.E.J. et al. "Influence on periapical tissues of indigenous oral bacteria and necrotic pulp tissue in monkeys," *European Journal of Oral Sciences*, 1981, 89(6), pp. 475–484. Available at: <https://doi.org/10.1111/j.1600-0722.1981.tb01711.x>.
53. Nagendrababu V, Murray P, Ordinola-Zapata R, Peters O, Rôças I, Siqueira J, Priya E, Jayaraman J, Pulikkotil S, Camilleri J, Boutsoukis C, Rossi-Fedele G. and Dummer P, 2021. PRILE 2021 guidelines for reporting laboratory studies in Endodontology: A consensus-based development. *International Endodontic Journal*, 2021, 54(9), pp.1482-1490.
54. Ng YL, Mann V, Gulabivala K. A prospective study of the factors affecting outcomes of nonsurgical root canal treatment: part 1: periapical health. *Int Endod J.* 2011; 44(7):583-609. doi: 10.1111/j.1365-2591.2011.01872.x. Epub 2011 Mar 2. PMID: 21366626.
55. Ng YL, Mann V, Rahbaran S, Lewsey J, Gulabivala K. Outcome of primary root canal treatment: systematic review of the literature -- Part 2. Influence of clinical factors. *Int Endod J.* 2008; 41(1):6-31. doi: 10.1111/j.1365-2591.2007.01323.x. Epub 2007 Oct 10. PMID: 17931388.
56. Nouroloyouni A. et al. "Single cone obturation versus cold lateral compaction techniques with bioceramic and resin sealers: Quality of obturation and push-out bond strength," *International Journal of Dentistry*, 2023, pp. 1–8. Available at: <https://doi.org/10.1155/2023/3427151>.

57. Nouroloyouni, A. et al. "Single cone obturation versus cold lateral compaction techniques with bioceramic and resin sealers: Quality of obturation and push-out bond strength," *International Journal of Dentistry*, 2023, pp. 1–8. Available at: <https://doi.org/10.1155/2023/3427151>.
58. Okabe T, Sakamoto M, Takeuchi H. and Matsushima K. Effects of pH on Mineralization Ability of Human Dental Pulp Cells. *Journal of Endodontics*, 2006, 32(3), pp.198-201.
59. Okiji T, Yoshiba K. Reparative dentinogenesis induced by mineral trioxide aggregate: a review from the biological and physicochemical points of view. *Int J Dent*. 2009; doi: 10.1155/2009/464280.
60. Özata, F. et al. "A comparative study of apical leakage of apexit, KETAC-endo, and diaket root canal sealers," *Journal of Endodontics*, 1999, 25(9), pp. 603–604. Available at: [https://doi.org/10.1016/s0099-2399\(99\)80317-3](https://doi.org/10.1016/s0099-2399(99)80317-3).
61. Poggio C, Trovati F, Ceci M, Colombo M, Pietrocola G. Antibacterial activity of different root canal sealers against *Enterococcus faecalis*. *J Clin Exp Dent*. 2017; 9(6):e743-e748. doi: 10.4317/jced.53753. PMID: 28638549; PMCID: PMC5474328.
62. Price R. and Roulet J. The value of consensus conferences: Peer review by 50 key opinion leaders! *Stomatology EDU Journal*, 2018, 5(4), pp.202-204.
63. Rathi C, et al. "Functions of Root Canal Sealers- A Review," *Jemds.com Review Article J. Evolution Med. Dent. Sc*, 2020, 9(17), pp. 2278–4748.
64. Reeves R, Stanley HR. The relationship of bacterial penetration and pulpal pathosis in carious teeth. *Oral Surg Oral Med Oral Pathol*. 1966; 22(1):59-65. doi: 10.1016/0030-4220(66)90143-5. PMID: 5220026.

65. Reszka P, Nowicka A, Dura W, Marek E. and Lipski, M. SEM and EDS study of TotalFill BC Sealer and GuttaFlow Bioseal root canal sealers. *Dental and Medical Problems*, 2019, 56(2), pp.167-172.
66. Rickert U, Dixon C. The controlling of root surgery. *Congres Dentaire International 1931*: 15-22.
67. Rodríguez-Lozano F, Collado-González M, Tomás-Catalá C, García-Bernal D, López S, Oñate-Sánchez R, Moraleda J and Murcia L. GuttaFlow Bioseal promotes spontaneous differentiation of human periodontal ligament stem cells into cementoblast-like cells. *Dental Materials*, 2019, 35(1), pp.114-124.
68. Saygili G, Saygili S, Tuglu I, Davut Capa I. In vitro cytotoxicity of GuttaFlow Bioseal, GuttaFlow 2, AH-Plus and MTA Fillapex. *Iran Endod J* 2017; 12:354–9.
69. Schroeder A. *Endodontics--science and practice: a textbook for student and practitioner*. Quintessence Pub Co; 1981.
70. Silva E, Rosa T, Herrera D, Jacinto R, Gomes B. and Zaia A, Evaluation of Cytotoxicity and Physicochemical Properties of Calcium Silicate-based Endodontic Sealer MTA Fillapex. *Journal of Endodontics*, 2013, 39(2), pp.274-277.
71. Siqueira JF Jr, Rôças IN. Clinical implications and microbiology of bacterial persistence after treatment procedures. *J Endod*. 2008; 34, pp.1291–301.
72. Siqueira JF, Jr, Rôças IN. Microbiology of endodontic infections. In: Hargreaves KM, Berman LB. editors. *Cohen's Pathways of the Pulp*. 11 ed. St. Louis, MO: Elsevier; (2016). p. 599–629.

73. Sjogren U, Hagglund B, Sundqvist G, Wing K. Factors affecting the long-term results of endodontic treatment. *J Endod.* 1990; 16(10): pp. 498-504. doi: 10.1016/S0099-2399(07)80180-4. PMID: 2084204.
74. Soares I, Goldberg F, Massone E, et al. Periapical tissue response to two calcium hydroxide containing endodontic sealers. *J Endod*, 1990; 16: pp. 166–9.
75. Souza L, Lopes J, Encarnação D, Mazali I, Martin R, Camilli J. and Bertran C. Comprehensive in vitro and in vivo studies of novel melt-derived Nb-substituted 45S5 bioglass reveal its enhanced bioactive properties for bone healing. *Scientific Reports*, 2018, 8(1).
76. Stoor P, Söderling E. and Salonen J. Antibacterial effects of a bioactive glass paste on oral microorganisms. *Acta Odontologica Scandinavica*, 1998, 56(3), pp.161-165.
77. Sundqvist G. Bacteriological studies of necrotic dental pulps , (1976)
78. Tabassum S, Khan FR. Failure of endodontic treatment: The usual suspects. *Eur J Dent.* 2016; 10:144–7.
79. Takadama, H. et al. “Mechanism of biomineralization of apatite on a sodium silicate glass: TEM–EDX study in vitro,” *Chemistry of Materials*, 2001, 13(3), pp. 1108–1113. Available at: <https://doi.org/10.1021/cm0008718>.
80. Tanomaru-Filho M, Torres F, Chávez-Andrade G, de Almeida M, Navarro L, Steier L. and Guerreiro-Tanomaru, J. Physicochemical Properties and Volumetric Change of Silicone/Bioactive Glass and Calcium Silicate–based Endodontic Sealers. *Journal of Endodontics*, 2017, 43(12), pp.2097-2101.
81. Väkiparta M, Forsback A, Lassila L, Jokinen M, Yli-Urpo A and Vallittu P, Biomimetic mineralization of partially bioresorbable glass fiber reinforced

- composite. *Journal of Materials Science: Materials in Medicine*, 2005, 16(9), pp.873-879.
82. Wallace KE, Hill RG, Pembroke JT, Brown CJ, Hatton PV. Influence of sodium oxide content on bioactive glass properties. *J Materials Science: Materials in Medicine* 1999; 10:697-701.
83. Wallace K. and Hill R, Influence of sodium oxide content on bioactive glass properties. *Journal of Materials Science*, 1999, 10, pp.697-701.
84. Waltimo T.M.T. et al. "Clinical performance of 3 endodontic sealers," *Oral Surgery, Oral Medicine, Oral Pathology, Oral Radiology, and Endodontology*, 2001, 92(1), pp. 89–92. Available at: <https://doi.org/10.1067/moe.2001.116154>.
85. Washio A, Morotomi T, Yoshii S. and Kitamura C. Bioactive Glass-Based Endodontic Sealer as a Promising Root Canal Filling Material without Semisolid Core Materials. *Materials*, 2019, 12(23), p.3967.
86. Xiang, Y. and J. Du "Effect of strontium substitution on the structure of 45S5 bioglasses." *Chemistry of Materials*, 2011, 23(11): 2703-2717.
87. Yigit, Dilek & Gençoğlu, Nimet. Evaluation of resin / silicone based root canal sealers. Part I: Physical properties. *Digest Journal of Nanomaterials and Biostructures*, 2012, 7.

SECTION 14 – APPENDICES

Appendix 1 –

Paired Samples Statistics for radiopacity for the commercial and novel sealant from the Statistical Product and Service Solutions software (SPSS)

	Mean	N	Std. Deviation	Std. Error Mean
Pair 1 GFB	4.0806	18	.36534	.08611
Novel	5.5428	18	.41339	.09744

Paired Samples Correlations			
	N	Correlation	Sig.
Pair 1 GFB & Novel	18	-.177	.483

Paired Samples Test				
	Paired Differences			
	Mean	Std. Deviation	Std. Error Mean	95% Confidence Interval of the Difference

				Lower	Upper
Pair 1	GFB - Novel	-1.46222	.59812	.14098	-1.75966 -1.16478

Paired Samples Test

		t	df	Sig. (2-tailed)
Pair 1	GFB - Novel	-10.372	17	.000